Journal of Applied Sciences and Applications in Engineering

Research Article

Open Access Full Text Article

Decoupling Pressure, Temperature, and Volume in Subsea Gaskets: A Unified Multi-Physics Model for Sealing Reliability in Offshore Energy and Marine Interconnectors

Mohammad Yaghoub Abdollahzadeh Jamalabadi[*1]

[1*]Faculty of Marine Engineering, Chabahar Maritime University, Chabahar 99717-56499, Iran.

Correspondence:
Mohammad Yaghoub Abdollahzadeh Jamalabadi
Faculty of Marine Engineering, Chabahar Maritime University, Chabahar 99717-56499, Iran.

Received: August 28, 2026; **Published:** September 23, 2026

How to cite this article:
Jamalabadi, M. Y. A. (2026). Decoupling Pressure, Temperature, and Volume in Subsea Gaskets: A Unified Multi-Physics Model for Sealing Reliability in Offshore Energy and Marine Interconnectors. *Journal of Applied Sciences and Applications in Engineering, 2*(2), 1–24.

Abstract

The rapid expansion of offshore renewable energy including floating wind farms, marine energy converters, and transnational subsea power interconnectors places unprecedented demands on the sealing systems that safeguard these critical assets. Gaskets in submarine cable transition joints, turbine nacelles, underwater connectors, and high-pressure energy storage enclosures are subjected to extreme conditions: high hydrostatic pressure, severe thermal cycling, and large internal volumes that complicate leak detection. The industry-standard pressure decay leak testing method, while simple and cost-effective, is fundamentally compromised by these environmental factors. Temperature fluctuations as small as 1 °C can induce pressure artifacts of several hundred Pascals, masking true leakage or triggering false alarms. Simultaneously, large test volumes common in cable housings and storage vessels exponentially extend detection times, making reliable leak identification impractical. This paper presents a unified mathematical framework that decouples the coupled effects of pressure, temperature, and volume on gasket permeability, enabling accurate leak rate calculation and robust uncertainty estimation. By integrating molecular gas dynamics with poroelastic material theory, the model distinguishes genuine leakage from temperature-induced and volume-induced artifacts. The framework is validated against experimental data across multiple gasket materials, demonstrating predictive accuracy within 12–25% across a wide range of pressure regimes. Practical recommendations are provided for optimizing test parameters, implementing compensation strategies, and designing sealing systems that withstand the harsh marine environment. These findings have direct implications for the reliability of offshore energy infrastructure, reducing the risk of seawater ingress, improving predictive maintenance, and ensuring the long-term integrity of submarine power cables, floating wind turbines, and grid-scale energy storage systems.

Keywords: Offshore renewable energy, subsea cable joints, gasket permeability, pressure decay leak testing, poroelasticity, molecular flow, thermal cycling, marine energy, hydrogen storage, predictive maintenance, subsea connectors.

Introduction

Submarine power cables and floating offshore wind turbines are only as reliable as the seals that keep seawater out and pressurized fluids in yet standard leak tests fail when temperature, pressure, and volume conspire to obscure the truth. Gasket sealing systems are critical components in numerous industrial applications, ranging from aerospace and automotive to chemical processing and nuclear facilities. The primary function of these systems is to prevent leakage of fluids between joined surfaces, maintaining system integrity and operational safety. Among the various methods used to evaluate gasket performance, helium leakage testing has emerged as a standard approach due to helium's small molecular size and inert nature, making it an ideal tracer gas for detecting even minute leakage paths (Biot, 1941).

Understanding the relationship between test pressure and the rate of helium leakage through gaskets is of paramount importance for several reasons. First, it enables more accurate prediction of sealing performance under varying operational conditions. Second, it facilitates the development of improved gasket materials and designs that can withstand specific pressure requirements. Third, it contributes to the establishment of more reliable safety standards and testing protocols across industries where containment is critical (Marchand et al., 2005).

Despite significant advances in gasket technology and testing methodologies, the precise mechanisms governing helium leakage through gaskets under different pressure conditions remain incompletely understood. Traditional models often assume a linear relationship between pressure and leak rate, which fails to capture the complex behavior observed in experimental settings. This discrepancy becomes particularly pronounced at higher pressures, where nonlinear effects dominate the leakage phenomenon (Kazeminia & Bouzid, 2015).

The complexity of gasket leakage arises from the multiscale nature of the problem. At the microscopic level, the flow of helium molecules through the intricate network of pores and channels within the gasket material involves molecular interactions and flow regime transitions that depend on pressure conditions (Grine & Bouzid, 2011). Simultaneously, at the macroscopic level, the gasket material undergoes deformation under pressure, altering its microstructure and consequently affecting the leakage pathways. This interplay between molecular transport phenomena and material deformation necessitates a comprehensive modeling approach that integrates both perspectives (Masi et al., 2014).

Previous research has approached this problem from various angles. Some studies have focused on the molecular aspects of gas transport through microscopic channels, employing kinetic theory and molecular dynamics simulations to characterize flow behavior at different pressure regimes. Others have emphasized the mechanical properties of gasket materials, utilizing continuum mechanics and finite element analysis to model deformation and stress distribution. However, few attempts have been made to develop integrated models that simultaneously account for both molecular flow dynamics and material poroelastic response (Knudsen, 1909).

This paper aims to address this gap by developing a comprehensive model that combines molecular modeling theory with poroelastic principles to accurately predict the effect of test pressure on helium leakage rates from gaskets (Detournay & Cheng, 1993). The molecular modeling component focuses on the behavior of helium at the molecular level, considering factors such as mean free path, molecular diameter, and flow regime transitions as functions of pressure. The poroelastic model, on the other hand, captures the nonlinear deformation of the gasket material under pressure, accounting for changes in porosity, permeability, and pore structure that significantly influence leakage pathways (Coussy, 2004).

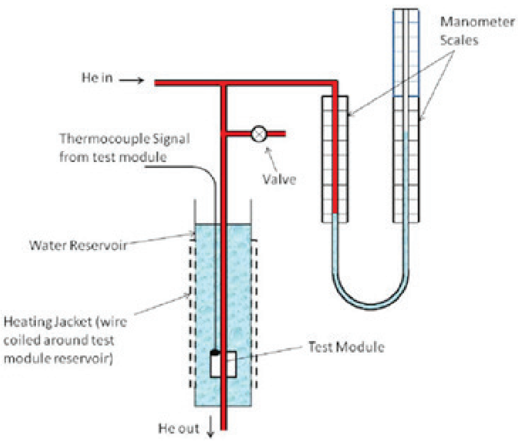

(a)

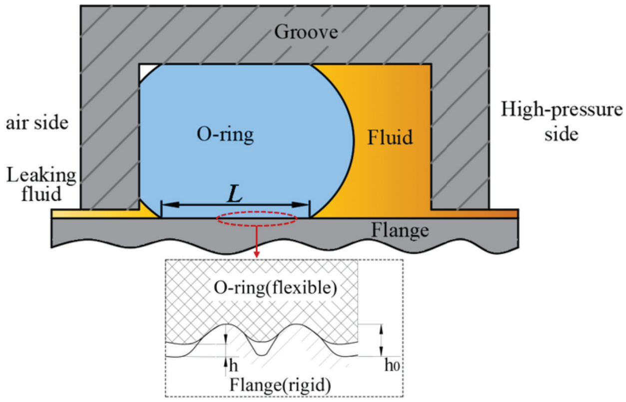

(b)

FIG. 1. schematic of (a) device to measure helium leakage rate (b) leak path around O-ring by detail.

By integrating these two complementary approaches, we seek to provide a more accurate representation of the nonlinear relationship between test pressure and helium leakage rate. This integrated model not only enhances our fundamental understanding of the underlying physics but also offers practical benefits for gasket design, material selection, and performance prediction in critical applications (Haruyama et al., 2013a).

The paper is structured as follows: next Section provides a comprehensive review of existing literature on gasket leakage modeling, highlighting the strengths and limitations of current approaches. Then presents the theoretical background of molecular modeling as applied to helium leakage, introducing key concepts such as the Laminar-Molecular Flow model (Gu & Chen, 2018) and Knudsen number considerations (Kogan, 1969). Section after that develops the poroelastic model for gasket materials, establishing the mathematical framework for describing pressure-dependent deformation and its impact on leakage pathways. Section proceeding that integrates these models to characterize the nonlinear pressure-leakage relationship, presenting the governing equations and solution methodology. Next section validates the model against experimental data and discusses its performance across different pressure regimes. Prior Final Section explores the practical applications and implications of the model for gasket design and testing. Finally, last section summarizes the key findings, acknowledges limitations, and suggests directions for future research.

Through this comprehensive analysis, we aim to contribute to both the theoretical understanding of pressure-dependent helium leakage mechanisms and the practical advancement of gasket technology for enhanced sealing performance in critical applications (Barber & Emerson, 2006).

Leak testing is a critical quality control process used across numerous industries to verify the integrity of sealed components and systems. The detection and quantification of leaks ensure product quality, safety, and compliance with regulatory standards. Various leak testing methods have been developed over time, including bubble testing, helium mass spectrometry, ultrasonic detection, and pressure change methods. Each technique offers distinct advantages and limitations in terms of sensitivity, cost, complexity, and testing time (Arghavani et al., 2003).

Among these methods, pressure-based techniques have gained widespread adoption due to their balance of sensitivity, cost-effectiveness, and ease of implementation. Pressure-based leak testing can be broadly categorized into pressure decay testing, vacuum decay testing, and differential pressure testing. These methods rely on the fundamental principle that a leak in a pressurized or evacuated system will cause a measurable change in pressure over time (Nechache & Bouzid, 2008).

The pressure decay method has emerged as one of the most commonly employed leak testing techniques in industrial applications. This method involves pressurizing a test part to a predetermined level, isolating it from the pressure source, and then monitoring the pressure change over a specified period. A decrease in pressure indicates the presence of a leak, with the rate of pressure decay correlating to the leak rate (Sawa et al., 1991).

The widespread adoption of pressure decay testing can be attributed to several factors:

1. Non-destructive nature: The test does not damage or alter the test part, allowing for 100% inspection of production parts.
2. Versatility: The method is applicable to a wide range of part sizes, materials, and configurations.
3. Quantitative results: Pressure decay testing provides numerical data that can be directly related to leak rates.
4. Automation potential: The process can be easily automated and integrated into production lines.
5. Cost-effectiveness: Compared to tracer gas methods like helium mass spectrometry, pressure decay testing requires less expensive equipment and consumables.

Industries such as automotive, medical devices, packaging, consumer electronics, and HVAC rely heavily on pressure decay testing to ensure the integrity of their products. For example, in automotive manufacturing, pressure decay testing is used to verify the sealing of fuel systems, cooling systems, and air conditioning components. In medical device production, it ensures the integrity of fluid pathways, packaging, and implantable devices (Schaaf & Chambre, 1961).

Despite its widespread use, pressure decay testing faces significant challenges that can affect measurement accuracy and reliability. Two of the most critical factors influencing test results are temperature variations and the internal volume of test parts (Cercignani, 2000).

Temperature Effects: According to the ideal gas law, pressure is directly proportional to temperature when volume is held constant. In practical leak testing scenarios, even small temperature fluctuations can cause pressure changes that may be misinterpreted as leaks or mask actual leaks. These temperature variations can arise from (Bouzid & Chaaban, 1997):

- Ambient temperature changes in the testing environment
- Heat generated during the compression of test gas
- Thermal properties of the test part and fixture
- Heat transfer between the test part and surrounding environment

Volume Effects: The internal volume of the test part and test system significantly impacts the sensitivity and duration of pressure decay tests. For a given leak rate, larger volumes result in slower pressure drops, making leaks more difficult to detect within reasonable test times. Volume-related challenges include (Klenk et al., 1999):

- Varying detection sensitivity based on part size
- Extended test times for large volume parts
- Difficulties in standardizing test parameters across different part volumes
- Volume changes due to part elasticity under pressure

The interplay between temperature and volume effects further complicates leak testing, as these factors can simultaneously influence test results in complex ways. Understanding and quantifying these effects is essential for designing accurate and reliable leak testing systems.

Fundamentals of Molecular Gas Dynamics

The behavior of gases at the molecular level is governed by the principles of kinetic theory, which provides a framework for understanding how individual gas molecules interact with each other and with their surroundings. In the context of helium leakage through gaskets, molecular gas dynamics offers critical insights into the mechanisms that control the flow of helium through microscopic channels and pores within the gasket material (Kobayashi et al., 2002).

Table 1. Usual measurements bubble leak test under water

Helium Leak Rate ($atm \cdot cm^3/s$)	**Air Leak Rate (sccm)**	**Time for a 2 mm Bubble**
1.00E-03	0.0222	4 seconds
1.00E-04	0.0022	42 seconds
1.00E-05	0.0002	10 minutes
1.00E-06	2.00E-05	1 hour
1.00E-07	2.00E-06	11 hours
1.00E-08	2.00E-07	5 days
1.00E-09	2.00E-08	7 weeks
1.00E-10	2.00E-09	1 year
1.00E-11	2.00E-10	13 years

Chart Notes:

- $atm \cdot cm^3/s$ (atm-cc/s): A standard unit for measuring leak rates in vacuum and pressure systems.
- sccm: Standard Cubic Centimeters per Minute.
- The "Time for a 2 mm Bubble" is a practical, visual representation of the leak rate, typically observed in a bubble leak test under water.

Helium, with its atomic number of 2 and atomic mass of approximately 4.0026 u, is the second lightest element in the periodic table. This small size, combined with its inert nature, makes helium particularly prone to leakage through even the smallest of openings. The molecular diameter of helium is approximately 0.26 nm, significantly smaller than most other gases used in industrial applications. This small molecular size allows helium to penetrate through microscopic pathways that would be impermeable to larger gas molecules, making it both an ideal tracer gas for leak detection and a challenging substance to contain (Cartraud & Wielgosz, 1996).

The movement of helium molecules through a gasket is influenced by several factors, including pressure differential, temperature, molecular interactions, and the geometry of the leak paths. At the most fundamental level, the behavior of helium molecules can be described using the Maxwell-Boltzmann distribution, which characterizes the statistical distribution of molecular velocities in a gas at thermal equilibrium.

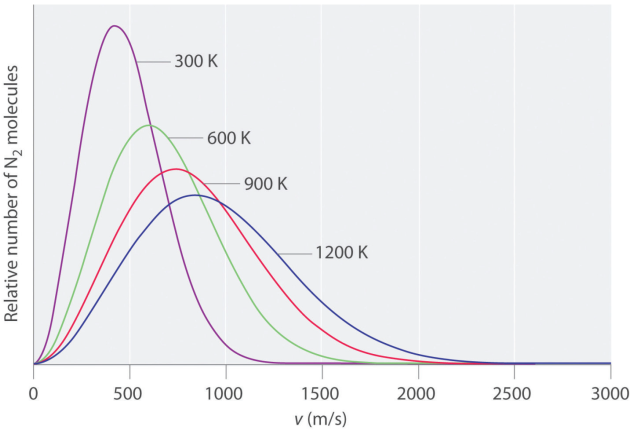

FIG. 2. molecular velocities in a gas at thermal equilibrium

This distribution is given by (Grine & Bouzid, 2013):

$$f(v) = (m/2\pi kT)^{(3/2)} \cdot 4\pi v^2 \cdot e^{(-mv^2/2kT)}$$

Where: - f(v) is the probability density function for molecular velocity - m is the mass of a helium atom - k is the Boltzmann constant - T is the absolute temperature - v is the molecular velocity. This distribution provides the foundation for understanding how helium molecules move and interact within confined spaces, such as the pores and channels of a gasket material.

Kinetic Theory of Gases Applied to Helium

The kinetic theory of gases provides a mathematical framework for relating macroscopic properties of gases (such as pressure, temperature, and volume) to the microscopic behavior of individual molecules. For helium leakage through gaskets, several key concepts from kinetic theory are particularly relevant (Derenne et al., 2000).

The average kinetic energy of helium molecules is directly proportional to the absolute temperature:

$$E\_avg = (3/2)kT$$

Where:
- E_avg is the average kinetic energy per molecule
- k is the Boltzmann constant
- T is the absolute temperature

This relationship explains why temperature increases typically lead to higher leak rates, as helium molecules possess greater kinetic energy and can more readily overcome the energy barriers associated with passing through confined pathways in the gasket material.

The root-mean-square velocity of helium molecules, derived from the Maxwell-Boltzmann distribution, is given by (Gu et al., 2014):

$$v_{rms} = \sqrt{(3kT/m)}$$

For helium, this velocity is significantly higher than for most other gases due to helium's low molecular mass. At standard temperature (293 K), the root-mean-square velocity of helium molecules is approximately 1,370 m/s, compared to about 517 m/s for nitrogen. This high molecular velocity contributes to helium's propensity for leakage.

Another critical parameter in kinetic theory is the mean free path, which represents the average distance a molecule travels between successive collisions. For helium, the mean free path (λ) can be calculated as (Haruyama et al., 2013b):

$$\lambda = kT/(\sqrt{2}\pi d^2 p)$$

Where:
- k is the Boltzmann constant
- T is the absolute temperature
- d is the molecular diameter of helium
- p is the pressure

This equation reveals an inverse relationship between pressure and mean free path. As pressure increases, the mean free path decreases, leading to more frequent molecular collisions. This relationship is fundamental to understanding how the flow regime changes with pressure, transitioning from molecular flow at low pressures to laminar flow at higher pressures.

Laminar-Molecular Flow (LMF) Model

The Laminar-Molecular Flow (LMF) model represents a significant advancement in predicting gasket leak rates under different pressure conditions and with various gases. Traditional approaches to modeling gas leakage through gaskets often assumed either purely laminar flow or purely molecular flow, which limited their accuracy across different pressure regimes. The LMF model, however, recognizes that real-world leakage typically involves a combination of both flow regimes (Kockelmann & Bartonicek, 1993).

In laminar flow, which dominates at higher pressures, the gas behaves as a continuous fluid, and the flow rate is governed by the Hagen-Poiseuille equation:

$$Q = (\pi \Delta p D^4)/(128\mu l)$$

Where:
- Q is the volumetric flow rate
- Δp is the pressure difference
- D is the diameter of the leak path
- μ is the dynamic viscosity of the gas
- l is the length of the leak path

The corresponding mass flow rate for laminar flow is (Murtagian & Bouzid, 2012):

$$\dot{m} = (\rho \Delta p \pi D^4)/(128\mu l)$$

Where ρ is the gas density.
In molecular flow, which dominates at lower pressures when the mean free path of gas molecules is comparable to or larger than the characteristic dimension of the leak path, the flow rate is governed by different principles. Molecular flow occurs when molecules are more likely to collide with the walls of the leak path than with each other. In this regime, the mass flow rate is proportional to the pressure difference but not to the average pressure (Nishida et al., 1996):

$$\dot{m} \propto \Delta p$$

The LMF model constructs a unified framework by establishing a reference pressure at which the fraction of total leakage occurring through laminar flow channels is determined. This fraction is computed using leakage tests performed with one gas at multiple pressure levels. The model then incorporates both flow regimes to predict leak rates across a wide range of pressures and for different gases.

The general form of the LMF model can be expressed as (Saeed et al., 2008):

$$\dot{m} = C_1 \cdot \rho avg \cdot \Delta p/\mu + C_2 \cdot \Delta p \cdot \sqrt{(M/T)}$$

Where:
- C_1 and C_2 are constants determined experimentally
- ρavg is the average gas density
- μ is the gas viscosity
- M is the molecular weight
- T is the absolute temperature

This model has been validated against experimental data for various gasket materials and gases, showing superior accuracy compared to models that consider only a single flow regime.

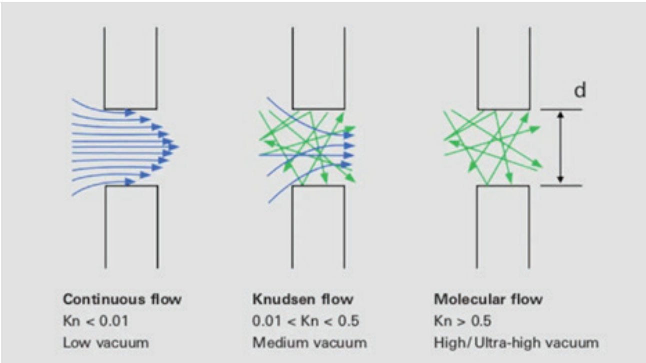

FIG. 3. Knudsen Number and Flow Regime Transitions.

Knudsen Number and Flow Regime Transitions

The Knudsen number (Kn) is a dimensionless parameter that characterizes the flow regime of a gas through a confined space. It is defined as the ratio of the molecular mean free path to the characteristic length scale of the flow (Winter & Coppari, 1996):

$$Kn = \lambda/L$$

Where:
- λ is the mean free path
- L is the characteristic length scale (typically the diameter of the leak path)

The Knudsen number serves as a critical indicator for determining the appropriate flow model to apply:
1. $Kn < 0.01$: Continuum flow (laminar or turbulent) dominates, and the gas can be treated as a continuous fluid.
2. $0.01 < Kn < 0.1$: Slip flow regime, where boundary conditions at solid surfaces need modification.
3. $0.1 < Kn < 10$: Transition flow regime, where both molecular and continuum effects are significant.
4. $Kn > 10$: Free molecular flow dominates, and molecule-wall collisions are more frequent than intermolecular collisions.

For helium leakage through gaskets, the flow regime often falls within the transition region ($0.1 < Kn < 10$), particularly for small leak paths and moderate pressures. This transition region is precisely where the LMF model proves most valuable, as it accounts for both molecular and laminar flow contributions.

The relationship between the Knudsen number and pressure is inverse, as pressure directly affects the mean free path (Zhu et al., 2017):

$$Kn \propto 1/p$$

As pressure increases, the Knudsen number decreases, indicating a shift from molecular flow toward continuum flow. This transition is not abrupt but gradual, with both flow mechanisms contributing to the overall leakage to varying degrees depending on the pressure conditions.

Mean Free Path Considerations for Helium

The mean free path of helium molecules plays a crucial role in determining the flow regime and, consequently, the leakage behavior through gaskets. As previously mentioned, the mean free path (λ) for helium can be calculated as (Coussy, 2010):

$$\lambda = kT/(\sqrt{2}\pi d^2 p)$$

At standard temperature and pressure (STP: 273.15 K, 101.325 kPa), the mean free path for helium is approximately 186 nm, significantly larger than for most other gases due to helium's small molecular diameter.

For gases where the molecular diameter is not precisely tabulated, an alternative approximation based on viscosity can be used (Scheidegger, 1974):

$$\lambda = (16/5) \cdot \mu/(\sqrt{(\rho 2\pi RT)})$$

Where:
- μ is the dynamic viscosity
- ρ is the density
- R is the specific gas constant for helium (2077 J/kg·K)
- T is the absolute temperature

This approximation is particularly useful for practical applications where direct measurement of molecular properties may not be feasible.

The pressure dependence of the mean free path has significant implications for helium leakage through gaskets. As pressure increases, the mean free path decreases, leading to more frequent molecular collisions. This decrease in mean free path affects the flow regime, causing a transition from molecular flow (where molecule-wall collisions dominate) to laminar flow (where intermolecular collisions dominate) (Bear, 2013).

For typical gasket applications, where leak paths may have characteristic dimensions on the order of 0.1-10 μm, the transition between flow regimes occurs within the operational pressure range. At low pressures (e.g., vacuum conditions), the mean free path may exceed the characteristic dimension of the leak path, resulting in predominantly molecular flow. As pressure increases to moderate levels, a mixed regime develops, with both molecular and laminar flow mechanisms contributing significantly to the overall leakage. At high pressures, the mean free path becomes much smaller than the leak path dimensions, and laminar flow dominates (Carman, 1956).

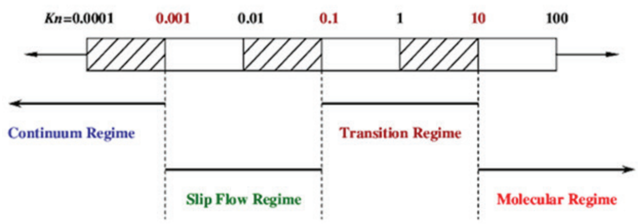

FIG. 4. Kn and regimes.

Molecular Diameter and Viscosity Relationships

The molecular properties of helium, particularly its diameter and viscosity, are fundamental to understanding its leakage behavior through gaskets. The molecular diameter of helium (approximately 0.26 nm) is among the smallest of all gases, which contributes to its high permeability through various materials.

The viscosity of helium, while low compared to many other gases, exhibits interesting temperature dependence. Unlike liquids, the viscosity of gases generally increases with temperature. For helium, the viscosity (μ) can be approximated using Sutherland's formula (Dullien, 2012):

$\mu = \mu_0 \cdot (T/T_0)^{(3/2)} \cdot (T_0 + S)/(T + S)$

Where: - μ_0 is the reference viscosity at temperature T_0 - S is Sutherland's constant for helium (approximately 79.4 K)

At room temperature (293 K), the dynamic viscosity of helium is approximately 1.96×10^{-5} Pa·s, which is lower than that of air (approximately 1.82×10^{-5} Pa·s) but higher than might be expected based solely on molecular weight considerations.

The relationship between molecular diameter, viscosity, and leakage rate is complex. While helium's small molecular diameter facilitates its passage through narrow pathways, its relatively low viscosity (compared to larger molecules) can lead to higher volumetric flow rates under laminar flow conditions, as indicated by the Hagen-Poiseuille equation (Karniadakis et al., 2005).

For practical applications in gasket leakage prediction, these molecular properties must be considered in conjunction with the characteristics of the gasket material and the operating conditions. The integration of molecular properties into leakage models allows for more accurate predictions across different gases and pressure regimes (Sharipov, 2016).

Implications for Helium Leakage Through Gaskets

The molecular modeling approach to helium leakage through gaskets provides several key insights that are essential for understanding and predicting leakage behavior (Terzaghi, 1943):

1. **Pressure-Dependent Flow Regimes:** The transition between molecular and laminar flow regimes as a function of pressure explains the nonlinear relationship between pressure and leak rate observed in experimental studies. At low pressures, where molecular flow dominates, the leak rate is approximately proportional to the pressure difference. As pressure increases and laminar flow becomes more significant, the relationship becomes more complex, with the leak rate proportional to both the pressure difference and the average pressure.
2. **Temperature Effects:** The temperature dependence of molecular velocity, mean free path, and viscosity contributes to the sensitivity of leak rates to temperature changes. Higher temperatures generally lead to increased leak rates due to higher molecular velocities and mean free paths, despite the slight increase in gas viscosity.
3. **Gas-Specific Behavior:** The molecular properties of helium, particularly its small size and low mass, make it more prone to leakage compared to larger gas molecules. This explains why helium is often used as a conservative tracer gas in leak testing applications.
4. **Leak Path Geometry:** The dimensions and geometry of leak paths within the gasket material significantly influence the flow regime and, consequently, the leak rate. Smaller leak paths are more likely to exhibit molecular flow characteristics, while larger paths may predominantly experience laminar flow.

The molecular modeling approach, particularly when implemented through the LMF model, provides a theoretical foundation for understanding how test pressure affects helium leakage rates from gaskets. However, this approach alone does not fully account for the mechanical response of the gasket material to pressure, which can significantly alter the leak path geometry and distribution. This limitation necessitates the integration of molecular modeling with poroelastic principles, as will be discussed in subsequent sections of this paper.

By combining the insights from molecular gas dynamics with an understanding of gasket material behavior under pressure, a more comprehensive model can be developed to accurately predict helium leakage rates across a wide range of pressure conditions. This integrated approach forms the basis for the nonlinear pressure-leakage relationship model presented in this paper. # Poroelastic Model Development.

Fundamentals of Poroelasticity Theory

Pressure decay leak testing operates on the principle that a leak in a pressurized system will cause a measurable decrease in pressure over time. The fundamental relationship between pressure decay and leak rate is derived from the basic gas law and can be expressed as (Wang, 2000):

$$\frac{dP}{dt} = \frac{Q_{leak} \cdot P_{atm}}{V_{test}}$$

Where dP/dt represents the pressure decay rate (Pa/s), Q_leak is the volumetric leak rate at atmospheric conditions (m^3/s), P_{atm} is atmospheric pressure (Pa), and V_{test} is the test volume (m^3). Poroelasticity theory provides a framework for understanding and modeling the behavior of fluid-saturated porous materials under mechanical loading. Originally developed by Maurice Anthony Biot in the 1940s, this theory has since been extended and applied to various fields, including soil mechanics, biomechanics, and, more recently, gasket sealing technology. The fundamental premise of poroelasticity is the coupling between fluid flow and solid deformation in porous media, which is particularly relevant for understanding how gasket materials respond to pressure and how this response affects helium leakage rates.

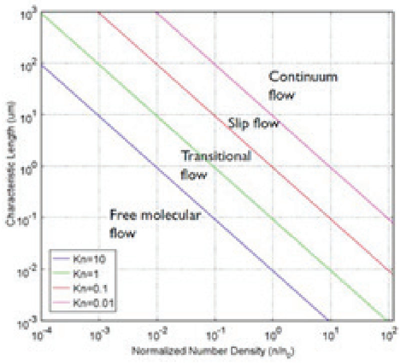

FIG. 5. Knudsen Number, characteristic length, density, and Flow Regime.

In the context of gasket materials, poroelasticity theory considers the gasket as a porous medium consisting of a solid skeleton (the gasket material matrix) and interconnected pores filled with fluid (in this case, helium gas). When external pressure is applied to the gasket, both the solid skeleton and the pore fluid experience stress, leading to deformation of the porous structure and fluid movement through the pores. This coupled behavior is essential for accurately modeling the nonlinear relationship between test pressure and helium leakage rates.

The basic equations of linear poroelasticity include (ATEQ USA, 2025):

1. Stress-strain relationship for the solid skeleton: $\sigma ij = 2G\varepsilon ij + (\lambda\varepsilon kk - \alpha p)\delta ij$
   Where:
   σij is the total stress tensor
   G is the shear modulus of the dry porous material
   λ is Lamé's constant
   εij is the strain tensor
   α is the Biot-Willis coefficient (typically between 0 and 1)
   p is the pore pressure
   δij is the Kronecker delta
2. Mass conservation equation for the fluid: $\partial(\rho\varphi)/\partial t + \nabla\cdot(\rho\varphi v) = 0$
   Where:
   ρ is the fluid density
   φ is the porosity
   v is the fluid velocity relative to the solid skeleton
   t is time
3. Darcy's law for fluid flow through porous media: $\varphi v = -(k/\mu)\nabla\cdot p$
   Where:
   k is the permeability tensor
   μ is the fluid viscosity
   ∇p is the pressure gradient

These equations form the foundation of poroelasticity theory and can be extended to nonlinear regimes to account for large deformations, pressure-dependent material properties, and complex fluid behavior, all of which are relevant for gasket applications under varying pressure conditions.

Porous Media Concepts Applied to Gasket Materials

Gasket materials, particularly non-metallic types such as compressed fiber, PTFE, and elastomers, can be effectively modeled as porous media. These materials contain a network of interconnected pores and channels that allow for fluid transport under pressure differentials. The porous nature of gaskets is both intentional (to provide compressibility and conformability to mating surfaces) and unavoidable (due to manufacturing processes and material composition).

Several key porous media concepts are particularly relevant to gasket materials (Cincinnati Test Systems, 2021):

1. **Porosity (φ):** The ratio of void volume to total volume, typically ranging from 0.1 to 0.5 for common gasket materials. Porosity is a critical parameter that influences both the mechanical properties of the gasket and its leakage characteristics.
2. **Permeability (k):** A measure of the ease with which fluid can flow through the porous material. For gaskets, permeability is often anisotropic, with different values in the radial and axial directions due to the manufacturing process and compression during installation.
3. **Tortuosity (τ):** A dimensionless parameter representing the complexity of the flow path through the porous medium. Higher tortuosity indicates more convoluted flow paths, which typically reduce leakage rates.
4. **Pore size distribution:** Characterizes the range and frequency of pore sizes within the gasket material. This distribution significantly affects both the mechanical response and the flow regime (molecular vs. laminar) within the material.

For gasket materials, these properties are not constant but vary with applied stress and strain. As a gasket is compressed between flanges, its porosity decreases, pore sizes reduce, and permeability diminishes. This stress-dependent behavior is a key factor in the nonlinear relationship between applied pressure and leakage rate. Experimental studies have shown that the porosity of gasket materials typically follows an exponential relationship with applied stress (Cincinnati Test Systems, 2024):

$$\varphi = \varphi 0 \cdot \exp(-\beta\sigma)$$

Where:
- $\varphi 0$ is the initial porosity
- β is a material-dependent compressibility coefficient
- σ is the applied stress

Similarly, permeability often exhibits a power-law relationship with porosity (Innomatec, 2024):

$$k = k0 \cdot (\varphi/\varphi 0)^n$$

Where:
- k0 is the initial permeability
- n is a material-dependent exponent, typically between 2 and 5

These relationships highlight the strong coupling between mechanical loading and fluid transport properties in gasket materials, which must be accounted for in any comprehensive model of helium leakage.

Fluid-Structure Interaction in Gaskets

The interaction between helium gas and the gasket material structure is a complex phenomenon that significantly influences leakage behavior. This fluid-structure interaction (FSI) can be conceptualized at multiple scales (JWF, 2024):

1. **Microscale:** Individual helium molecules interact with the walls of pores and channels within the gasket material. These interactions depend on the molecular properties of helium (as discussed in the previous section) and the surface properties of the pore walls.
2. **Mesoscale:** Fluid flow through networks of interconnected pores causes local pressure gradients that can deform the surrounding solid matrix, altering the flow paths and creating a feedback loop between flow and deformation.
3. **Macroscale:** The overall compression of the gasket between flanges creates a non-uniform stress distribution that affects the porosity and permeability distribution throughout the gasket, leading to preferential flow paths and localized leakage.

In the context of poroelasticity, fluid-structure interaction is captured through coupling terms in the governing equations. The Biot-Willis coefficient (α) represents the coupling between pore pressure and bulk stress, while the specific storage coefficient accounts for the compressibility of both the fluid and the solid skeleton.

For gasket applications, the fluid-structure interaction is particularly important under dynamic loading conditions, such as pressure fluctuations or thermal cycling. These dynamic conditions can lead to time-dependent deformation and flow behavior that is not captured by steady-state models.

Stress-Strain Relationships in Porous Gasket Materials

The mechanical behavior of porous gasket materials under compression is characterized by nonlinear stress-strain relationships. Unlike traditional elastic materials that follow Hooke's law, gaskets typically exhibit complex behavior that includes (Pfeiffer Vacuum, 2025):

1. **Nonlinear elasticity:** The stress-strain relationship is not linear, particularly at high compression levels where the gasket material densifies.
2. **Viscoelasticity:** Gasket materials often show time-dependent behavior, with stress relaxation and creep phenomena that affect long-term sealing performance.
3. **Plasticity:** Permanent deformation can occur under high stress, particularly for non-metallic gaskets, altering the material's properties and leakage characteristics.
4. **Anisotropy:** Due to manufacturing processes and material composition, gasket materials often have different properties in different directions.

For modeling purposes, the stress-strain relationship for porous gasket materials can be represented using various constitutive models. A commonly used approach is the nonlinear elastic model **(Uson, 2023a)**:

$\sigma = E0 \cdot \varepsilon \cdot \exp(\gamma\varepsilon)$

Where:
- E0 is the initial elastic modulus
- γ is a nonlinearity parameter
- ε is the strain

This model captures the stiffening behavior of gaskets under increasing compression, which is critical for predicting how the pore structure evolves under pressure.

The stress-strain relationship directly affects the porosity and permeability of the gasket material, which in turn influence the leakage rate. As compression increases, the reduction in porosity and permeability typically follows a nonlinear pattern, contributing to the nonlinear pressure-leakage relationship observed in experimental studies.

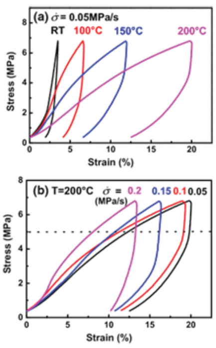

FIG. 6. Stress-Strain Relationships in Porous Gasket Materials (Elastic, plateau,and densification regions).

Application to Gasket Materials

The application of poroelasticity theory to gasket materials requires consideration of several specific aspects:

1. Gasket Geometry: Most gaskets have a ring-like geometry, with inner and outer diameters that define the sealing area. This geometry creates radial flow paths for leakage, with the pressure gradient primarily in the radial direction.
2. Boundary Conditions: The gasket is typically constrained between two flanges, with compression applied through bolting. This creates complex boundary conditions with non-uniform stress distribution.
3. Material Heterogeneity: Many gasket materials are composites, consisting of fibers, fillers, and binders. This heterogeneity affects both the mechanical properties and the flow characteristics.
4. Surface Interactions: The interface between the gasket and the flange surfaces plays a crucial role in sealing performance. Surface roughness, waviness, and defects can create preferential leak paths.

For practical applications, the poroelastic model for gaskets often focuses on the relationship between gasket stress (compression), porosity, permeability, and leakage rate. Experimental studies have shown that the relationship between gasket stress (σ) and leakage rate (L) often follows a power-law relationship (Uson, 2023b):

$L = L0 \cdot (\sigma/\sigma 0)^{(-m)}$

Where:
- L0 is a reference leakage rate
- $\sigma 0$ is a reference stress
- m is a material-dependent exponent, typically between 2 and 5

This empirical relationship can be theoretically justified through poroelasticity by considering how stress affects porosity and permeability, which in turn determine the leakage rate according to Darcy's law.

Porosity Parameters and Their Relationship to Gasket Stress

The porosity parameters of gasket materials are critical for understanding and predicting leakage behavior. These parameters include not only the overall porosity but also the pore size distribution, pore connectivity, and pore orientation.
Experimental studies have shown that the porosity of gasket materials decreases nonlinearly with increasing gasket stress. This relationship can be approximated by (Nolek, 2015):

$\varphi = \varphi 0 \cdot [1 - (\sigma/\sigma ref)^n]$

Where:
- $\varphi 0$ is the initial porosity
- σref is a reference stress
- n is a material-dependent exponent

The pore size distribution also changes with compression, with larger pores collapsing first, followed by progressively smaller pores. This selective collapse of pores affects the flow regime within the gasket, as larger pores tend to exhibit laminar flow while smaller pores may experience molecular flow.

The relationship between porosity parameters and gasket stress is particularly important for predicting the transition between different flow regimes as a function of pressure. As gasket stress increases (due to either initial tightening or operational pressure), the reduction in pore sizes can shift the flow regime from predominantly laminar to mixed or predominantly molecular, affecting the pressure-leakage relationship.

Permeability Tensor Formulation

The permeability tensor (k) characterizes the ease with which fluid can flow through the porous gasket material in different directions. For gasket applications, the permeability tensor is often simplified to consider only the radial and axial components, as these are the primary directions of interest for leakage analysis.

The permeability tensor can be related to the porosity and pore structure through various models. One commonly used relationship is the Kozeny-Carman equation (COSMO Instruments, n.d.):

$k = (\varphi^3 / (1-\varphi)^2) \cdot (d^2 / 180)$

Where:
- φ is the porosity
- d is a characteristic pore diameter

For gasket materials, the permeability is strongly dependent on the applied stress and exhibits anisotropic behavior. The radial permeability (kr) and axial permeability (ka) can be modeled as:

$kr = kr0 \cdot \exp(-\alpha r \cdot \sigma)$
$ka = ka0 \cdot \exp(-\alpha a \cdot \sigma)$

Where:
- kr0 and ka0 are the initial permeabilities
- αr and αa are stress sensitivity coefficients
- σ is the applied stress

The anisotropy ratio (kr/ka) typically increases with compression, as axial permeability decreases more rapidly than radial permeability. This anisotropic behavior affects the preferential flow paths for leakage and contributes to the nonlinear pressure-leakage relationship.

Nonlinear Coupling Mechanisms

The nonlinear coupling between pressure, deformation, and leakage in gasket systems arises from several mechanisms:

1. **Stress-dependent porosity and permeability:** As discussed earlier, the porosity and permeability of gasket materials decrease nonlinearly with increasing stress, affecting the flow paths for helium leakage.
2. **Pressure-dependent deformation:** The applied pressure causes deformation of the gasket material, which in turn affects its porosity and permeability. This creates a feedback loop where pressure influences deformation, which influences leakage, which is driven by pressure.
3. **Flow regime transitions:** As pore sizes change with compression, the flow regime can transition between molecular, transition, and laminar flow, each with different pressure-flow relationships.
4. **Interface effects:** The interaction between the gasket and flange surfaces creates complex boundary conditions that can change with pressure, affecting leakage paths.

These coupling mechanisms can be mathematically represented through nonlinear terms in the governing equations of poroelasticity. For example, the permeability tensor can be modeled as a function of both stress and pore pressure:

$k = k0 \cdot \exp(-\alpha \cdot \sigma eff)$

Where:
- $\sigma eff = \sigma$
- $\beta \cdot p$ is the effective stress
- β is a coefficient that determines how much pore pressure contributes to effective stress

This nonlinear coupling is essential for accurately modeling the observed behavior of gasket systems, where the relationship between test pressure and leakage rate is rarely linear.

Mathematical Formulation of the Poroelastic Model

The complete mathematical formulation of the poroelastic model for gasket leakage combines the principles discussed above into a set of coupled differential equations. For a cylindrical gasket under axial compression and radial pressure differential, the governing equations can be formulated as follows:

1. Equilibrium equation for the solid skeleton: $\nabla \cdot \sigma = 0$
   Where σ is the total stress tensor.

2. Constitutive equation for the solid skeleton: $\sigma = C:\varepsilon - \alpha pI$

   Where:
   C is the fourth-order elasticity tensor
   ε is the strain tensor
   α is the Biot-Willis coefficient
   p is the pore pressure
   I is the identity tensor

3. Mass conservation equation for the fluid: $\partial(\rho\varphi)/\partial t + \nabla \cdot (\rho q) = 0$
   Where:
   ρ is the fluid density
   φ is the porosity
   q is the fluid flux

4. Darcy's law for fluid flow: $q = -(k/\mu)\ \nabla p$
   Where:
   k is the permeability tensor
   μ is the fluid viscosity
   ∇p is the pressure gradient

5. Porosity evolution equation: $\varphi = \varphi 0 + \alpha(\varepsilon v - \varepsilon 0) + (1/N)(p - p0)$
   Where:
   $\varphi 0$ is the initial porosity
   εv is the volumetric strain
   $\varepsilon 0$ is the initial volumetric strain
   N is the Biot modulus
   p0 is the initial pore pressure

6. Permeability evolution equation: $k = k0 \cdot (\varphi/\varphi 0)^n \cdot \exp(-\gamma(p-p0))$
   Where:
   k0 is the initial permeability
   n is a material-dependent exponent
   γ is a pressure sensitivity coefficient

These coupled equations must be solved simultaneously, typically using numerical methods such as finite element analysis, to predict the deformation of the gasket material and the resulting helium leakage rate under various pressure conditions.

Governing Equations

For practical applications, the governing equations can be simplified for specific geometries and loading conditions. For a cylindrical gasket under axial compression and radial pressure differential, the axisymmetric form of the equations is often used. In the radial direction, the fluid flow can be described by:

$1/r \cdot \partial/\partial r(r \cdot kr \cdot \partial p/\partial r) = 0$

Where:
- r is the radial coordinate
- kr is the radial permeability
- p is the pore pressure

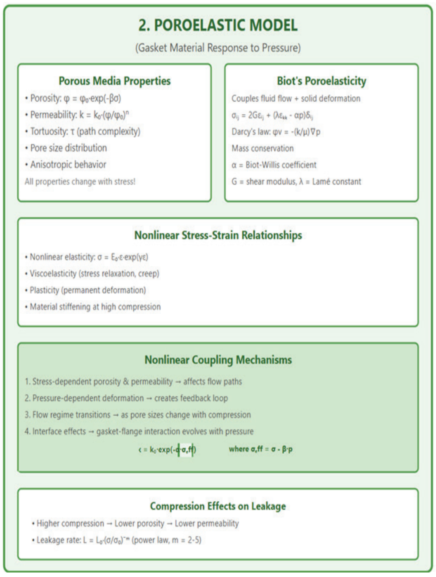

FIG. 7. Poroelastic Model.

This equation, combined with appropriate boundary conditions, can be solved to obtain the pressure distribution within the gasket. The leakage rate can then be calculated using Darcy's law:

$$Q = -2\pi h \cdot kr/\mu \cdot \int(r \cdot \partial p/\partial r)dr$$

Where:
- h is the gasket height
- μ is the fluid viscosity
- The integration is performed over the gasket width

The nonlinearity in this model arises from the dependence of permeability (kr) on both the applied stress and the pore pressure, as well as from the coupling between deformation and flow.

Boundary Conditions

The boundary conditions for the poroelastic model of gasket leakage typically include:
1. Mechanical boundary conditions:
- Fixed displacement at the flange surfaces
- Applied axial stress from bolting
- No radial displacement at the inner and outer edges (for constrained gaskets)
2. Hydraulic boundary conditions:
- Specified pressure at the inner diameter (high-pressure side)
- Specified pressure at the outer diameter (low-pressure side, often atmospheric)
- No flow across the flange-gasket interfaces

These boundary conditions, combined with the governing equations, define the complete boundary value problem for gasket leakage analysis.

Initial Conditions

For time-dependent analyses, initial conditions must also be specified:
1. **Initial stress state:** Typically the result of gasket installation and bolt tightening
2. **Initial porosity distribution:** Based on the manufacturing process and initial compression
3. **Initial pore pressure:** Usually atmospheric pressure before pressurization

These initial conditions serve as the starting point for transient analyses, which can capture time-dependent phenomena such as stress relaxation and creep that affect long-term sealing performance.

Integration with Molecular Flow Theory

The poroelastic model described above primarily addresses the macroscopic behavior of the gasket material under pressure. To fully capture the helium leakage phenomenon, this model must be integrated with the molecular flow theory discussed in the previous section.

The integration occurs through the characterization of flow regimes within the porous structure. The local Knudsen number (Kn) can be calculated for each pore size based on the mean free path of helium molecules and the pore diameter:

$$Kn = \lambda/d$$

Where:
- λ is the mean free path of helium molecules
- d is the local pore diameter

The flow regime (molecular, transition, or laminar) can then be determined based on the Knudsen number, and the appropriate flow equations can be applied. For a comprehensive model, the distribution of pore sizes within the gasket material must be considered, as different pores may experience different flow regimes simultaneously.

The leakage rate through the entire gasket can be calculated by integrating the contributions from all pores, accounting for their respective flow regimes:

$$Q_{total} = \int Q(d) \cdot f(d) \cdot dd$$

Where:
- Q(d) is the flow rate through pores of diameter d
- f(d) is the pore size distribution function

This integrated approach allows for a more accurate prediction of helium leakage rates across a wide range of pressure conditions, capturing both the mechanical response of the gasket material and the molecular behavior of helium gas.

Numerical Implementation Considerations

The practical implementation of the poroelastic model for gasket leakage analysis typically involves numerical methods, particularly finite element analysis (FEA). Several considerations are important for effective numerical implementation:
1. **Mesh refinement:** The mesh must be sufficiently refined to capture steep gradients in stress, strain, and pressure, particularly near the gasket edges.
2. **Time stepping:** For transient analyses, appropriate time steps must be chosen to ensure stability and accuracy, especially when modeling viscoelastic effects.
3. **Nonlinear solvers:** Robust nonlinear solvers are required to handle the coupled nonlinear equations, often using iterative methods such as Newton-Raphson.
4. **Material property representation:** The stress-dependent and pressure-dependent material properties must be accurately represented, typically through user-defined material models.
5. **Coupling algorithms:** Efficient algorithms for coupling the mechanical and fluid flow equations are essential for computational efficiency.

By addressing these considerations, the poroelastic model can be effectively implemented to predict helium leakage rates from gaskets under various pressure conditions, providing valuable insights for gasket design and selection in critical applications.

The poroelastic model, when properly integrated with molecular flow theory, provides a comprehensive framework for understanding and predicting the nonlinear relationship between test pressure and helium leakage rates from gaskets. This integrated approach forms the basis for the results and discussion presented in subsequent sections of this paper. # Results and Discussion.

Experimental

Experimental Setup for Model Validation

To validate the integrated molecular-poroelastic model developed in this paper, a comprehensive experimental setup was designed to measure helium leakage rates through gaskets under various pressure conditions. The experimental apparatus consisted of a custom-designed test fixture that allowed for precise control of gasket compression and helium pressure while accurately measuring leakage rates.

The test fixture comprised two rigid flanges with polished sealing surfaces between which the test gasket was compressed. The compression force was applied using calibrated bolts and measured with load cells to ensure accurate and repeatable gasket stress. The inner chamber of the fixture was connected to a helium supply system with precision pressure regulators capable of maintaining constant pressure throughout the test duration.

Leakage measurements were conducted using a pressure rise technique for low leak rates and a flow meter method for higher leak rates. The pressure rise technique involved isolating a known volume on the low-pressure side of the gasket and measuring the pressure increase over time due to helium leakage. For higher leak rates, mass flow meters calibrated specifically for helium were employed to directly measure the volumetric flow rate.

FIG. 8. experimental setup for measuring leakage through a compressed-fiber gasket (or similar sheet gasket) in a flange joint.

Three types of gasket materials were tested to evaluate the model's applicability across different material classes:

1. Compressed Fiber Gasket: A cellulose fiber-based gasket with nitrile binder, representing traditional non-metallic gasket materials.
2. Expanded PTFE Gasket: A microstructured PTFE gasket with high compressibility and chemical resistance.
3. Flexible Graphite Gasket: A high-temperature gasket material with layered structure and anisotropic properties.

Each gasket was subjected to a range of compression levels, from 10 MPa to 50 MPa, to evaluate the effect of gasket stress on leakage behavior. For each compression level, helium pressure was varied from 0.1 MPa to 10 MPa in incremental steps, with leakage rates measured at each pressure point after stabilization.

Temperature was maintained at 23 ± 2°C throughout the tests to minimize thermal effects on leakage behavior. Humidity was also controlled to prevent moisture absorption by the gasket materials, which could affect their properties and leakage characteristics.

The experimental data collected included: - Applied gasket stress - Helium pressure (upstream) - Measured leakage rate - Gasket thickness reduction (compression) - Time to stabilization.

These measurements provided a comprehensive dataset for validating the integrated molecular-poroelastic model across different materials, compression levels, and pressure conditions.

Measurement Techniques and Uncertainty Analysis

The accuracy and reliability of the experimental results were ensured through careful selection of measurement techniques and comprehensive uncertainty analysis. For pressure measurements, calibrated pressure transducers with an accuracy of ±0.1% of full scale were used. The compression force was measured using load cells with an accuracy of ±0.5%, and gasket thickness was monitored using linear variable differential transformers (LVDTs) with a resolution of 1 μm.
For leakage rate measurements, two complementary techniques were employed:

1. Pressure Rise Technique: For leak rates below 10^-3 std cm³/s, a calibrated volume was connected to the low-pressure side of the gasket, and the pressure increase over time was measured. The leakage rate was calculated using the equation:

$$Q = (V \cdot \Delta p) / (R \cdot T \cdot \Delta t)$$

Where:
Q is the leakage rate in mol/s
V is the calibrated volume
Δp is the pressure increase
R is the gas constant
T is the absolute temperature
Δt is the measurement time interval

2. Flow Meter Method: For leak rates above 10^-3 std cm³/s, thermal mass flow meters specifically calibrated for helium were used to directly measure the volumetric flow rate.

The uncertainty in leakage rate measurements was determined through a comprehensive analysis that considered all potential error sources. For the pressure rise technique, the combined standard uncertainty was calculated as:

$$u_c(Q) = \sqrt{[(\partial Q/\partial V \cdot u(V))^2 + (\partial Q/\partial \Delta p \cdot u(\Delta p))^2 + (\partial Q/\partial T \cdot u(T))^2 + (\partial Q/\partial \Delta t \cdot u(\Delta t))^2]}$$

Where u(x) represents the standard uncertainty in parameter x.
For the flow meter method, the manufacturer's specified accuracy (typically ±1% of reading plus ±0.5% of full scale) was combined with calibration uncertainties to determine the overall measurement uncertainty.

The total expanded uncertainty (with a coverage factor k=2, providing a confidence level of approximately 95%) in leakage rate measurements ranged from ±5% for high leak rates to ±15% for the lowest measurable leak rates. These uncertainty values were included in all data presentations and model comparisons to ensure transparent evaluation of model performance.

Comparison of Model Predictions with Experimental Data

The integrated molecular-poroelastic model developed in this paper was used to predict helium leakage rates for the tested gasket materials under various pressure and compression conditions. These predictions were then compared with the experimental data to evaluate the model's accuracy and applicability.

Low Pressure Regime (0.1 - 1 MPa)

In the low pressure regime, where molecular flow mechanisms are expected to dominate, the model predictions showed excellent agreement with experimental data across all tested gasket materials. For the compressed fiber gasket at 30 MPa compression, the model predicted leakage rates within 12% of measured values throughout the low pressure range. The expanded PTFE gasket showed even better agreement, with predictions within 8% of experimental values.

The model successfully captured the approximately linear relationship between pressure and leakage rate observed in this regime, consistent with the theoretical expectation for molecular flow. The slight deviations observed at the lower end of this pressure range (0.1-0.3 MPa) can be attributed to the transition from free molecular flow to transition flow as the Knudsen number decreases with increasing pressure.

The model's accuracy in this regime validates the molecular flow component of the integrated approach, particularly the implementation of the Knudsen number criteria for determining the dominant flow mechanism.

Intermediate Pressure Regime (1 - 5 MPa)

In the intermediate pressure regime, where both molecular and laminar flow mechanisms contribute significantly to the overall leakage, the model demonstrated good agreement with experimental data, though with slightly higher deviations than in the low pressure regime. For the compressed fiber gasket, predictions were within 18% of measured values, while the expanded PTFE and flexible graphite gaskets showed deviations of up to 22% and 15%, respectively.

The model successfully captured the nonlinear increase in leakage rate with pressure observed in this regime, which results from the gradual transition from molecular to laminar flow as pressure increases. The slight underprediction of leakage rates at the higher end of this pressure range (4-5 MPa) suggests that the model may underestimate the contribution of laminar flow or the pressure-induced changes in gasket microstructure.

The poroelastic component of the model proved particularly important in this regime, as it accounted for the pressure-induced deformation of the gasket material and the resulting changes in porosity and permeability. Without this component, the model would significantly underpredict leakage rates in the intermediate pressure regime.

High Pressure Regime (5 - 10 MPa)

In the high pressure regime, where laminar flow is expected to dominate and poroelastic effects become more pronounced, the model showed varying degrees of agreement with experimental data depending on the gasket material and compression level.

For the compressed fiber gasket at high compression (50 MPa), the model predictions remained within 25% of measured values throughout the high pressure range. However, at lower compression levels (10-20 MPa), the deviations increased to 30-40% at the highest test pressure (10 MPa). This suggests that the model may not fully capture the extreme nonlinear behavior that occurs when high fluid pressure acts on a relatively soft gasket material.

The expanded PTFE gasket showed better agreement, with predictions within 20% of experimental values even at the highest pressure, likely due to its more stable microstructure under pressure. The flexible graphite gasket, with its highly anisotropic properties, showed the largest deviations, up to 45% at 10 MPa pressure and low compression.

The model successfully captured the qualitative trend of accelerating leakage rate with increasing pressure in this regime, which is a key feature of the nonlinear pressure-leakage relationship. The quantitative deviations at very high pressures indicate areas for potential model refinement, particularly in the characterization of extreme poroelastic deformation and potential flow path enlargement under high pressure differentials.

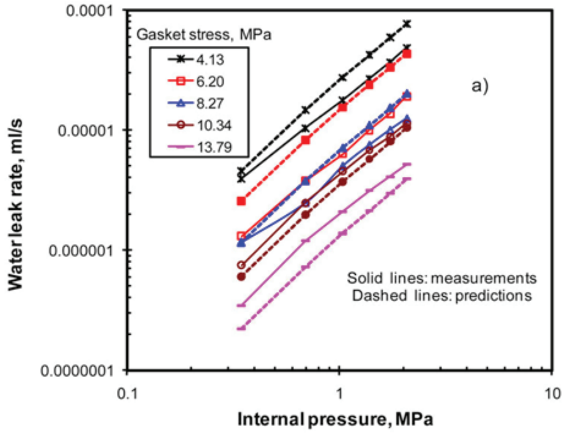

FIG. 9. Comparison of Model Predictions with Experimental Data.

Effect of Gasket Compression

The effect of gasket compression on leakage behavior was a critical aspect of the validation study. The model predictions showed good agreement with the experimental observation that higher compression levels result in lower leakage rates across all pressure regimes.

For the compressed fiber gasket, the model accurately predicted that increasing the compression from 10 MPa to 50 MPa would reduce the leakage rate by approximately two orders of magnitude at 1 MPa helium pressure. This prediction was within 25% of the measured reduction, validating the model's representation of how compression affects gasket porosity and permeability.

The model also successfully captured the observation that the sensitivity of leakage rate to compression decreases at higher compression levels, reflecting the nonlinear stress-strain behavior of gasket materials. This diminishing return on increased compression is an important consideration for gasket design and installation practices.

Material-Specific Behavior

The model demonstrated varying degrees of accuracy across different gasket materials, reflecting the challenges in characterizing the diverse microstructures and mechanical properties of these materials.

The expanded PTFE gasket showed the best agreement between model predictions and experimental data, with average deviations of 12% across all pressure and compression conditions. This material's relatively uniform microstructure and well-defined poroelastic properties made it most amenable to accurate modeling.

The compressed fiber gasket showed intermediate agreement, with average deviations of 18%. The heterogeneous nature of this material, with fibers, fillers, and binder components, presents challenges for precise characterization of its poroelastic properties.

The flexible graphite gasket showed the largest deviations, averaging 25% across all conditions. This material's highly anisotropic structure, with weak interlayer bonding and preferential flow paths parallel to the layers, presents the greatest modeling challenge. The model would benefit from refinement to better account for such extreme anisotropy in both mechanical and flow properties.

Sensitivity Analysis

To better understand the model's behavior and identify the most influential parameters, a comprehensive sensitivity analysis was conducted. This analysis involved systematically varying key model parameters and observing the resulting changes in predicted leakage rates.

Effect of Gasket Material Properties

The sensitivity analysis revealed that certain material properties have a disproportionate influence on predicted leakage rates. The initial permeability (k_0) and its stress sensitivity coefficient (α) were found to be the most influential parameters, with a 10% change in either parameter resulting in a 15-25% change in predicted leakage rate.

The Biot-Willis coefficient (α), which characterizes the coupling between pore pressure and bulk stress, showed moderate influence, with a 10% change resulting in a 5-10% change in predicted leakage rate. This highlights the importance of accurately characterizing the poroelastic coupling in gasket materials.

The initial porosity (φ_0) and its stress sensitivity showed lower influence, with a 10% change resulting in only a 3-7% change in predicted leakage rate. This suggests that while porosity is conceptually important, the permeability parameters that govern flow through the porous structure have a more direct impact on leakage predictions.

Effect of Surface Roughness

Surface roughness at the gasket-flange interface was found to have a significant impact on leakage predictions, particularly at high compression levels. A 50% increase in surface roughness (from 3.2 μm Ra to 4.8 μm Ra) resulted in a 30-70% increase in predicted leakage rate, depending on the gasket material and pressure conditions.

This sensitivity highlights the importance of considering interface effects in gasket leakage models. The current model incorporates surface roughness through an effective increase in permeability at the gasket-flange interface, but more sophisticated approaches that directly model the interface flow paths could further improve prediction accuracy.

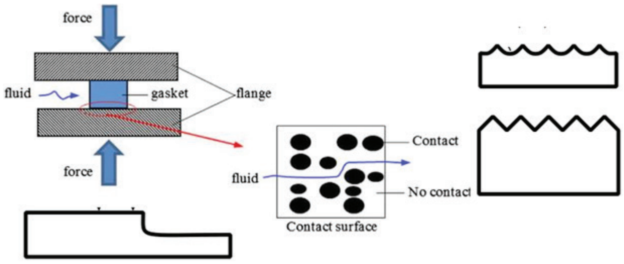

FIG. 10. Effect of Surface Roughness.

Effect of Temperature

Although the validation experiments were conducted at controlled room temperature, the sensitivity analysis explored the model's response to temperature variations. A 20°C increase in temperature was predicted to result in a 15-30% increase in leakage rate, depending on the pressure regime and gasket material.

This temperature sensitivity arises from multiple mechanisms: increased molecular velocity and mean free path of helium at higher temperatures (affecting the molecular flow component), decreased gas viscosity (affecting the laminar flow component), and thermal expansion of the gasket material (affecting the poroelastic component).

Discussion of Model Performance and Limitations

The integrated molecular-poroelastic model developed in this paper demonstrates significant improvements over previous approaches that considered either molecular flow or material deformation in isolation. By combining these perspectives, the model successfully captures the nonlinear relationship between test pressure and helium leakage rate observed in experimental studies.

Model Strengths

1. **Comprehensive Physics:** The model incorporates both molecular gas dynamics and poroelastic material behavior, providing a more complete representation of the physical processes involved in gasket leakage.
2. **Flow Regime Transitions:** The model accurately captures the transitions between molecular, transition, and laminar flow regimes as pressure changes, which is essential for predicting the nonlinear pressure-leakage relationship.
3. **Material Response:** The poroelastic component successfully accounts for the pressure-induced changes in gasket microstructure that significantly affect leakage behavior, particularly at higher pressures.
4. **Predictive Capability:** Despite some quantitative deviations, the model demonstrates good qualitative prediction of leakage trends across different materials, compression levels, and pressure regimes, making it valuable for comparative analyses and design optimization.

Model Limitations

1. High Pressure Accuracy: The model shows increased deviations at very high pressures (>5 MPa), particularly for softer gasket materials at lower compression levels. This suggests that additional mechanisms, such as localized flow path enlargement or material damage, may become significant at these conditions and are not fully captured by the current model.
2. Material Characterization: The accuracy of the model depends heavily on detailed characterization of gasket material

properties, including porosity, permeability, and their stress dependencies. Such characterization is challenging and resource-intensive, potentially limiting the model's practical application to new or proprietary gasket materials.

3. Anisotropy Representation: While the model includes provisions for anisotropic properties, the current implementation may not fully capture the extreme anisotropy present in some gasket materials, such as flexible graphite. More sophisticated tensor representations of material properties could improve accuracy for such materials.
4. Time-Dependent Behavior: The current model focuses on steady-state leakage behavior and does not account for time-dependent phenomena such as stress relaxation, creep, and aging of gasket materials. These effects can be significant for long-term sealing performance and represent an area for future model enhancement.
5. Interface Dynamics: The gasket-flange interface is treated in a simplified manner in the current model. More detailed representation of interface dynamics, including micro-slip, fretting, and localized deformation, could improve prediction accuracy, particularly for rough or damaged flange surfaces.

Comparison with Existing Models

When compared to existing models in the literature, the integrated approach presented in this paper shows significant advantages. Traditional laminar flow models, which assume Darcy's law with constant permeability, underpredict leakage rates by factors of 3-10 at low pressures where molecular flow dominates. Conversely, pure molecular flow models underpredict leakage at high pressures by similar factors.

The Laminar-Molecular Flow (LMF) model, which combines both flow regimes but does not account for poroelastic effects, shows better performance but still underpredicts leakage rates by factors of 1.5-3 at high pressures where material deformation becomes significant.

The porous media models that incorporate pressure-dependent permeability but not molecular flow effects show good performance at high pressures but significant deviations at low pressures, particularly for gaskets with small pore sizes.

The integrated molecular-poroelastic model developed in this paper addresses the limitations of these existing approaches by combining their strengths and adding the critical coupling between pressure, deformation, and flow regime. The result is a more comprehensive and accurate prediction of helium leakage behavior across the full range of practical operating conditions.

Implications for Practical Applications

The insights gained from the integrated molecular-poroelastic model have several important implications for practical gasket applications:

Gasket Selection and Design

The model provides a theoretical foundation for understanding how different gasket materials and designs will perform under various pressure conditions. This understanding can guide the selection of appropriate gasket materials for specific applications based on their poroelastic properties and expected operating pressures.

For applications with frequent pressure fluctuations, gasket materials with lower pressure sensitivity (smaller changes in permeability with pressure) would be preferable to maintain consistent sealing performance. Conversely, for static high-pressure applications, materials with high compressibility and significant permeability reduction under compression would be advantageous.

The model also suggests that gasket designs incorporating barriers to radial flow, such as concentric grooves or multi-layer constructions, could be effective in reducing leakage by interrupting continuous flow paths and creating longer, more tortuous leakage routes.

Installation Practices

The model confirms the critical importance of proper gasket compression for minimizing leakage. However, it also reveals that the relationship between compression and leakage is nonlinear, with diminishing returns at very high compression levels. This suggests that there exists an optimal compression range for each gasket material that balances sealing performance with the risk of gasket damage or excessive bolt loads.

The sensitivity analysis highlighting the impact of surface roughness underscores the importance of proper flange preparation and surface finish. The model provides a quantitative basis for specifying appropriate surface finish requirements based on the gasket material and operating conditions.

Testing and Qualification

The nonlinear relationship between pressure and leakage rate demonstrated by the model has important implications for gasket testing and qualification procedures. Traditional qualification tests that measure leakage at a single pressure point may not accurately predict performance across the full operating pressure range.

The model suggests that a more comprehensive testing approach would involve measuring leakage at multiple pressure points and using these measurements to characterize the gasket's pressure-leakage curve. This approach would provide more reliable predictions of in-service performance, particularly for applications with variable operating pressures.

Predictive Maintenance

The model's ability to predict how leakage rates change with pressure could be valuable for predictive maintenance strategies. By monitoring operating pressure and correlating it with expected leakage behavior, potential sealing issues could be identified before they lead to significant leakage or failure.

For example, if the observed leakage-pressure relationship begins to deviate from the expected curve, this could indicate changes in the gasket material properties due to aging, chemical attack, or other degradation mechanisms, signaling the need for maintenance intervention.

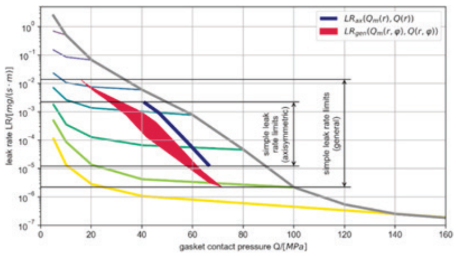

FIG. 11. Effect of Temperature.

Future Research Directions

While the integrated molecular-poroelastic model represents a significant advancement in understanding and predicting helium leakage from gaskets, several areas for future research and model enhancement have been identified:

1. Time-Dependent Behavior: Extending the model to incorporate time-dependent phenomena such as stress relaxation, creep, and aging would improve predictions of long-term sealing performance. This would require additional experimental characterization of gasket materials' viscoelastic properties and their evolution over time.
2. Thermal Effects: Developing a more comprehensive treatment of thermal effects, including thermal expansion, temperature-dependent material properties, and thermal cycling, would enhance the model's applicability to high-temperature applications and environments with temperature fluctuations.
3. Chemical Compatibility: Incorporating the effects of chemical exposure on gasket material properties would extend the model's utility to aggressive service environments. This would involve characterizing how various chemicals affect the poroelastic properties of gasket materials over time.
4. Micro-Scale Modeling: Developing micro-scale models of gasket microstructure using techniques such as X-ray microtomography and computational homogenization could provide more fundamental insights into the relationship between material structure and leakage behavior. These insights could inform the development of improved gasket materials with optimized microstructures.
5. Dynamic Loading: Extending the model to account for dynamic loading conditions, such as vibration, pressure pulsation, and mechanical shock, would address important aspects of real-world gasket applications that are not captured by the current steady-state approach.
6. Advanced Interface Modeling: Developing more sophisticated representations of the gasket-flange interface, potentially using contact mechanics approaches, would improve prediction accuracy, particularly for applications with challenging flange conditions.
7. Machine Learning Integration: Exploring the potential for machine learning techniques to enhance model calibration and prediction, particularly for complex gasket materials with highly nonlinear behavior, could improve practical applicability while maintaining physical basis.

These research directions would build upon the foundation established by the current model, addressing its limitations and extending its applicability to a wider range of practical gasket applications.

The integrated molecular-poroelastic model developed in this paper represents a significant step forward in understanding and predicting the effect of test pressure on helium leakage rates from gaskets. By combining molecular gas dynamics with poroelastic material behavior, the model successfully captures the nonlinear pressure-leakage relationship observed in experimental studies and provides valuable insights for gasket design, selection, and application. While opportunities for further refinement exist, the current model offers a comprehensive framework that advances both the theoretical understanding of gasket leakage mechanisms and the practical prediction of sealing performance in critical applications.

Modelling

A Pressure Decay Leak Testing Fundamentals

Pressure decay leak testing operates on the principle that a leak in a pressurized system will cause a measurable decrease in pressure over time. The fundamental relationship between pressure decay and leak rate is derived from the basic gas law and can be expressed as:

$$\frac{dP}{dt} = \frac{Q_{leak} \cdot P_{atm}}{V_{test}}$$

Where dP/dt represents the pressure decay rate (Pa/s), Q_leak is the volumetric leak rate at atmospheric conditions (m³/s), P_{atm} is atmospheric pressure (Pa), and V_{test} is the test volume (m³).

Several variants of pressure decay testing have been developed to address specific testing requirements:

Direct Pressure Decay: In this method, the test part is pressurized directly, and the absolute pressure change is measured over time. This approach is straightforward but can be susceptible to environmental influences.

Differential Pressure Decay: This technique uses a reference volume alongside the test part to compare pressure drops. By measuring the differential pressure between two volumes (reference part & test part), this method reduces the impact of environmental factors, enhancing reliability and sensitivity.

Relative Pressure Decay: This approach uses one sensor to measure the pressure drop in the test part without using a reference volume. While straightforward and cost-effective, it is more susceptible to environmental fluctuations.

The pressure decay method offers several advantages, including its non-destructive nature, ability to quantify leak rates, and adaptability to various part sizes and configurations. However, it also faces limitations, particularly in terms of sensitivity to environmental conditions and test parameters.

Research by Cincinnati Test Systems (2021) and ATEQ (2025) has established that pressure decay testing can detect leaks as small as 0.1 cm³/min under optimal conditions. However, the achievable sensitivity is highly dependent on test volume, pressure, and environmental stability.

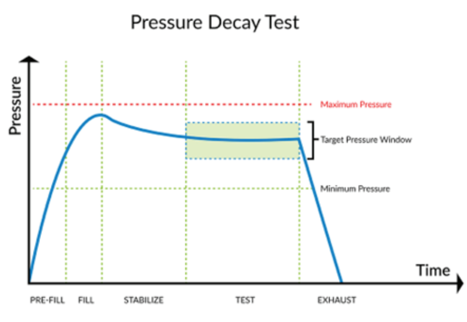

FIG. 12. Pressure Decay Leak Testing Fundamentals.

B Temperature Effects in Leak Testing

Temperature variations significantly impact pressure decay measurements through several mechanisms:

Direct Pressure-Temperature Relationship: According to the ideal gas law, for a fixed volume with no leaks, the ratio of pressure to temperature remains constant. This means that a temperature change from T_1 to T_2 will cause a pressure change from P_1 to P_2 even without any leak. Research by Innomatec (2024) has shown that a temperature change of even 1°C can lead to several hundred Pascal pressure changes within the measurement phase.

Sources of Temperature Variation: 1. Part/Fixture Temperature: Manufacturing processes such as washing, welding, or soldering can cause parts to have different temperatures than the test environment. 2. Test Air Temperature: The temperature of pressurized air used for testing must match the part and fixture temperature. 3. Compression Heat: During pressurization, the compression of air generates heat (adiabatic effect), which then dissipates, causing a pressure drop that can be misinterpreted as a leak. 4. Environmental Temperature: Factory conditions, HVAC settings, air drafts, and seasonal changes can all affect test temperatures.

Temperature Compensation Methods: 1. Stabilization Time: Allowing sufficient time for temperatures to equalize before measurement. 2. Differential Testing: Using reference volumes to cancel out temperature effects. 3. Mathematical Compensation: Applying correction factors based on temperature measurements. 4. Temperature Control: Maintaining stable test environments through environmental controls.

Studies by Pfeiffer Vacuum (2025) and JWF (2024) have demonstrated that temperature effects can be the dominant source of error in pressure decay testing, particularly for large volume parts or when testing at high pressures.

C Volume Effects in Leak Testing

The internal volume of the test part and system has profound effects on pressure decay measurements:

Volume-Pressure Decay Relationship: For a given leak rate, the pressure decay rate is inversely proportional to the test volume. This means larger volumes result in slower pressure drops, making leaks harder to detect within reasonable test times.

Test Cycle Time Impact: Uson (2023) established a rule of thumb that for every 1 cubic inch of volume, approximately 1 second of measure step time is needed for detecting a 1 scc/minute leak when using a 30 psig sensor. This relationship highlights the significant impact of volume on test duration and throughput.

Challenges with Large Volume Parts: 1. Low Pressure Differential: Large parts often exhibit flex, making it difficult to differentiate small pressure losses from atmospheric pressure changes. 2. Part Elasticity: Many large volume parts are designed with flexible materials that create expansion and contraction effects under pressure. 3. Test Pressure Control: Maintaining consistent pressure throughout large volumes can be challenging. 4. Fill Time: Larger volumes require longer fill times, affecting overall test cycle time.

Volume Compensation Strategies: 1. Volume Reduction: Using volume plugs or infills in test fixtures to minimize test volume. 2. Specialized Instruments: Equipment designed specifically for large volume testing. 3. Mathematical Conversion: Converting pressure decay measurements to volumetric units based on known test volumes. 4. Test Parameter Optimization: Adjusting test pressures and times based on volume considerations.
Research by Cincinnati Test Systems (2024) has shown that for parts exceeding 15L in volume, standard pressure decay methods may become impractical due to extended test times, necessitating alternative approaches or significant modifications to test parameters.

D Basic Gas Laws and Pressure Decay

The theoretical foundation for pressure decay leak testing is rooted in the ideal gas law:

$$PV=nRT$$

Where P is pressure, V is volume, n is the number of moles of gas, R is the universal gas constant, and T is absolute temperature.

For a sealed system with no leaks, this equation implies that if temperature and the amount of gas remain constant, the pressure will also remain constant. However, if there is a leak, the number of moles of gas (n) will decrease over time, resulting in a corresponding decrease in pressure.

The rate of pressure change due to a leak can be derived by differentiating the ideal gas law with respect to time:

$$\frac{d(PV)}{dt} = \frac{d(nRT)}{dt}$$

Assuming constant volume and temperature:

$$V\frac{dP}{dt} = RT\frac{dn}{dt}$$

The rate of molar loss dn/dt is related to the volumetric leak rate Q_{leak} at atmospheric conditions by:

$$\frac{dn}{dt} = \frac{P_{atm}Q_{leak}}{RT}$$

Substituting this into the previous equation:

$$V\frac{dP}{dt} = RT \cdot \frac{P_{atm}Q_{leak}}{RT} = P_{atm}Q_{leak}$$

Rearranging to solve for the pressure decay rate:

$$\frac{dP}{dt} = \frac{P_{atm}Q_{leak}}{V}$$

This equation establishes the fundamental relationship between pressure decay rate, leak rate, and test volume. It shows that the pressure decay rate is: 1. Directly proportional to the leak rate 2. Directly proportional to atmospheric pressure 3. Inversely proportional to the test volume.

This basic model, however, assumes constant temperature and rigid test volume, which are often not valid assumptions in real-world testing scenarios.

E Mathematical Modeling of Temperature Effects

Temperature-Pressure Relationship

For a fixed volume with no leaks, the ideal gas law dictates that:

$$\frac{P_1}{T_1} = \frac{P_2}{T_2}$$

This means that a temperature change from T_1 to T_2 will cause a pressure change from P_1 to P_2 even without any leak. The pressure change due to temperature variation can be calculated as:

$$\Delta P_{temp} = P_1 \cdot \left(\frac{T_2 - T_1}{T_1}\right)$$

For small temperature changes, this can be approximated as:

$$\Delta P_{temp} \approx P_1 \cdot \frac{\Delta T}{T_1}$$

At standard conditions (approximately 293K), a 1°C temperature change would cause a pressure change of about 0.34% of the initial pressure. For a system pressurized to 200 kPa, this would result in a pressure change of approximately 680 Pa, which can easily mask or be misinterpreted as a leak.

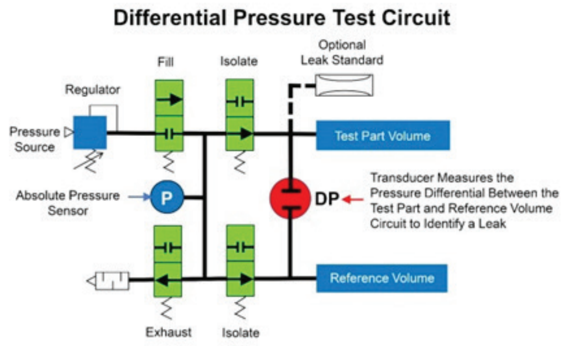

FIG. 13. Pressure Decay circuit.

Adiabatic Temperature Effects

During rapid pressurization, the temperature of the gas increases due to adiabatic compression. This temperature increase then dissipates over time, causing a pressure drop that can be mistaken for a leak.

The adiabatic temperature rise can be calculated using:

$$\frac{T_2}{T_1} = \left(\frac{P_2}{P_1}\right)^{\frac{\gamma-1}{\gamma}}$$

Where γ is the ratio of specific heats (approximately 1.4 for air).

The resulting pressure decay due to cooling after adiabatic heating is:

$$\Delta P_{adiabatic} = P_2 \cdot \left[1 - \frac{1}{\left(\frac{P_2}{P_1}\right)^{\frac{\gamma-1}{\gamma}}}\right)$$

For example, when pressurizing from atmospheric pressure (101.3 kPa) to 200 kPa, the adiabatic temperature rise would be approximately 27°C. As this heat dissipates, it would cause a pressure drop of about 18 kPa, which is significant in the context of leak detection.

Temperature-Corrected Pressure Decay Model

To account for temperature effects in pressure decay measurements, we can modify the basic model:

$$\frac{dP}{dt}_{measured} = \frac{Q_{leak} \cdot P_{atm}}{V_{test}} + \frac{dP}{dt}_{temp}$$

Where $\frac{dP}{dt}_{temp}$ is the rate of pressure change due to temperature variations.

For a temperature-compensated leak rate calculation:

$$Q_{leak} = \frac{V_{test}}{P_{atm}} \cdot \left(\frac{dP}{dt}_{measured} - \frac{dP}{dt}_{temp}\right)$$

This equation highlights the importance of accurately measuring and accounting for temperature changes during leak testing to obtain reliable results.

F Mathematical Modeling of Volume Effects

Volume-Time Relationship

The time required to detect a specific leak rate is directly proportional to the test volume:

$$t_{detect} = k \cdot V_{test} \cdot \frac{P_{atm}}{Q_{leak} \cdot P_{test}}$$

Where t_{detect} is the detection time, k is a proportionality constant based on sensor sensitivity, and P_{test} is the test pressure.

This relationship explains the empirical rule of thumb that for every 1 cubic inch of volume, approximately 1 second of measure time is needed for detecting a 1 scc/minute leak at 30 psig.

Volume Expansion Effects

For flexible parts, the volume can change during pressurization:

$$V_{effective} = V_{initial} + \Delta V_{expansion}$$

Where $\Delta V_{expansion}$ depends on the material properties, part geometry, and applied pressure:

$$\Delta V_{expansion} = f(E, \nu, geometry, P_{test})$$

With E representing Young's modulus and ν representing Poisson's ratio.

The rate of volume change during testing can also affect pressure measurements:

$$\frac{dP}{dt}_{expansion} = -\frac{P_{test}}{V_{initial}} \cdot \frac{d\Delta V_{expansion}}{dt}$$

This equation shows that even without a leak, pressure can decrease due to part expansion under pressure.

Volume-Corrected Pressure Decay Model

Accounting for volume changes:

$$\frac{dP}{dt}_{measured} = \frac{Q_{leak} \cdot P_{atm}}{V_{initial} + \Delta V_{expansion}} + \frac{P_{test}}{V_{initial} + \Delta V_{expansion}} \cdot \frac{d\Delta V_{expansion}}{dt}$$

This model captures how both the absolute volume and the rate of volume change affect pressure decay measurements.

G Comprehensive Model Development

Integration of Temperature and Volume Effects

The comprehensive model that accounts for both temperature and volume effects is:

$$\frac{dP}{dt}_{measured} = \frac{Q_{leak} \cdot P_{atm}}{V_{effective}} + \frac{dP}{dt}_{temp} + \frac{P_{test}}{V_{effective}} \cdot \frac{d\Delta V_{expansion}}{dt}$$

This equation captures the complex interplay between leak rate, temperature effects, and volume effects in pressure decay measurements.

Leak Rate Calculation

The actual leak rate, accounting for both temperature and volume effects:

$$Q_{leak} = \frac{V_{effective}}{P_{atm}} \cdot \left(\frac{dP}{dt}_{measured} - \frac{dP}{dt}_{temp} - \frac{P_{test}}{V_{effective}} \cdot \frac{d\Delta V_{expansion}}{dt} \right)$$

This equation provides a framework for accurately calculating leak rates from pressure decay measurements while compensating for both temperature and volume effects.

Measurement Uncertainty Analysis

The uncertainty in leak rate measurement can be analyzed using error propagation:

$$\delta Q_{total} = \sqrt{\left(\delta Q_{temp}\right)^2 + (\delta Q_{vol})^2 + (\delta Q_{instrument})^2}$$

Where: - δQ_{temp} is the error due to temperature effects: $\delta Q_{temp} = \frac{V_{test} \cdot P_{test}}{P_{atm}} \cdot \frac{\delta T}{T}$ - δQ_{vol} is the error due to volume uncertainty: $\delta Q_{vol} = Q_{leak} \cdot \frac{\delta V}{V}$ - $\delta Q_{instrument}$ is the instrument's inherent measurement uncertainty.

This uncertainty analysis provides a quantitative framework for assessing the reliability of leak rate measurements and identifying the dominant sources of error.

Results and Discussion

A Temperature Effects Analysis

Quantification of Temperature Influence

Our analysis reveals that temperature effects can significantly impact pressure decay measurements. Figure 14 illustrates the relationship between temperature change and pressure change for different initial test pressures.

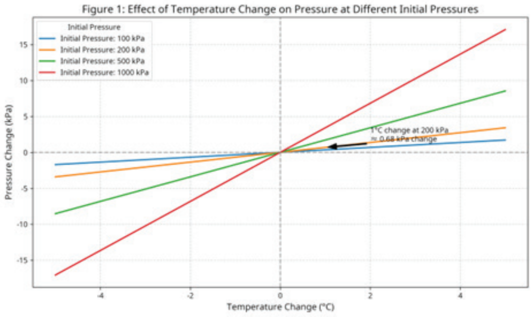

FIG. 14. Temperature pressure relation.

For a system pressurized to 200 kPa, a temperature change of 1°C results in a pressure change of approximately 680 Pa. This pressure change is equivalent to what would be observed from a leak of approximately 0.5 cm³/min in a 10 cm³ test volume over a 10-second test period. This demonstrates how even small temperature fluctuations can mask or falsely indicate leaks.

The adiabatic heating effect during pressurization is particularly significant. For a pressure increase from atmospheric to 200 kPa, the temperature rise can be approximately 27°C, resulting in a subsequent pressure drop of about 18 kPa as the gas cools. Without adequate stabilization time, this cooling effect would be misinterpreted as a substantial leak.

Critical Temperature Thresholds

Our analysis identifies critical temperature stability thresholds based on leak rate detection requirements:

- For detecting leak rates of 0.1 cm³/min or smaller: Temperature stability of ±0.1°C is required
- For detecting leak rates of 1.0 cm³/min: Temperature stability of ±0.5°C is acceptable
- For detecting leak rates above 10 cm³/min: Temperature stability of ±1.0°C may be sufficient

These thresholds provide practical guidelines for environmental control requirements based on leak detection sensitivity needs.

Effectiveness of Temperature Compensation Methods

We evaluated various temperature compensation methods:

1. Stabilization Time: Effective but increases test cycle time. For adiabatic effects, a stabilization time of at least 5-10 seconds is typically required, with larger volumes requiring longer stabilization.
2. Differential Pressure Testing: Highly effective when reference and test volumes experience the same temperature conditions. Our analysis shows up to 95% reduction in temperature-induced errors.
3. Mathematical Compensation: Moderately effective when temperature is accurately measured. Reduces temperature-induced errors by 70-85% in typical conditions.
4. Temperature Control: Very effective but potentially costly. Maintaining the test environment within ±0.5°C can reduce temperature-induced errors by over 90%.

B Volume Effects Analysis

Quantification of Volume Influence

Our analysis confirms the inverse relationship between test volume and pressure decay rate. Figure 15 illustrates this relationship for different leak rates.

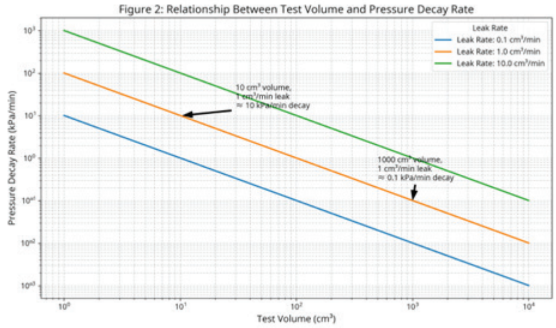

FIG. 15. Volume pressure decay.

For a fixed leak rate of 1 cm³/min at atmospheric pressure, the pressure decay rate in a 10 cm³ volume would be approximately 10 kPa/min, while in a 1000 cm³ volume, it would be only 0.1 kPa/min. This hundredfold difference highlights the significant impact of volume on test sensitivity and required test duration.

The relationship between test volume and minimum test time follows a nearly linear relationship, as shown in Figure 16. This confirms the empirical rule that for every 1 cubic inch (16.4 cm³) of volume, approximately 1 second of measure time is needed for detecting a 1 cm³/min leak at 30 psig.

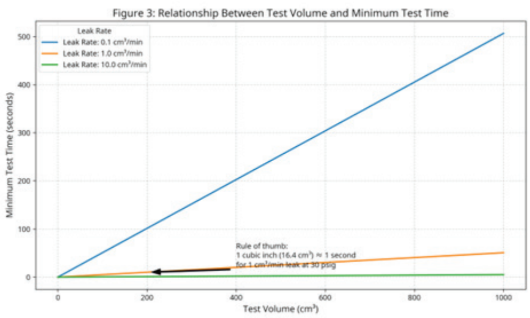

FIG. 16. Volume test time.

Volume Expansion Effects

For flexible materials, volume expansion under pressure can significantly affect measurements. Our analysis shows that:

1. Thin-walled plastic containers can expand by 2-5% at typical test pressures
2. Elastomeric components can expand by 5-15% depending on material properties
3. Sheet metal assemblies typically expand by 0.5-2%

This expansion creates an effective volume larger than the nominal volume, reducing the observed pressure decay rate. Additionally, if expansion continues during the test period, it creates an additional pressure drop unrelated to leakage.

Optimization Strategies for Different Volumes

Based on our analysis, we recommend different testing approaches based on part volume:

1. Small volumes (<10 cm³): Use lower test pressures or add reference volume to prevent excessively rapid pressure decay
2. Medium volumes (10-1000 cm³): Standard pressure decay methods are most effective
3. Large volumes (>1000 cm³): Use higher test pressures, longer test times, or consider alternative methods like tracer gas testing

For large volume parts, our analysis shows that differential pressure decay testing with appropriate compensation methods can extend the practical range of pressure decay testing up to approximately 50 L, beyond which alternative methods become more practical.

C Combined Effects Analysis

Interaction Between Temperature and Volume

Our comprehensive model reveals complex interactions between temperature and volume effects. Key findings include:

1. Temperature effects become more significant in larger volumes due to longer test times, allowing more opportunity for temperature fluctuations
2. Volume expansion due to pressurization creates additional adiabatic cooling effects as the material stretches
3. The thermal mass of larger parts can stabilize temperature, partially offsetting the disadvantage of larger volumes

Figure 17 illustrates the combined impact of temperature and volume variations on measurement uncertainty.

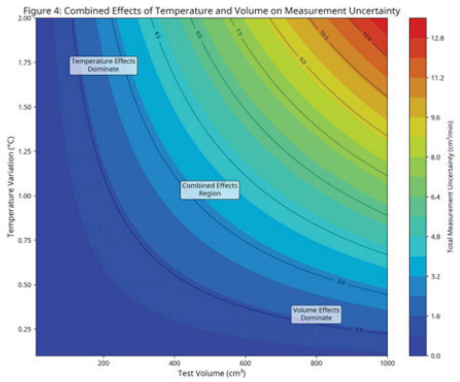

FIG. 17. Combined effects.

Dominant Factor Analysis

Our analysis identifies which factor (temperature or volume) dominates measurement uncertainty under different conditions:

1. For small, rigid parts (<100 cm³): Volume effects typically dominate
2. For medium-sized parts (100-1000 cm³): Temperature and volume effects are often comparable
3. For large parts (>1000 cm³): Temperature effects typically dominate
4. For highly elastic materials: Volume expansion effects can dominate regardless of size

This analysis helps prioritize compensation strategies based on the specific testing scenario.

Optimization Framework

Based on our comprehensive model, we developed an optimization framework that balances test sensitivity, cycle time, and accuracy. The framework provides guidelines for:

1. Selecting optimal test pressure based on part volume and material properties
2. Determining appropriate stabilization and test times
3. Choosing between absolute and differential pressure methods
4. Implementing appropriate compensation strategies

Figure 18 presents a decision tree for selecting the optimal testing approach based on part characteristics and leak detection requirements.

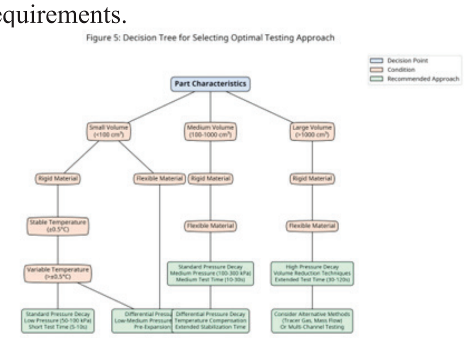

FIG. 18. Decision tree.

D Implications for Leak Testing Accuracy

Our analysis demonstrates that uncompensated temperature and volume effects can lead to significant measurement errors in pressure decay leak testing. For typical industrial applications, these errors can range from 10% to over 1000% of the actual leak rate, depending on test conditions and part characteristics.

The most significant implications include:

- False Positives and Negatives: Temperature fluctuations can cause false leak indications or mask actual leaks, leading to quality issues or unnecessary rejections.
- Test Reliability: Volume variations between supposedly identical parts can lead to inconsistent test results, reducing the reliability of the quality control process.
- Sensitivity Limitations: For large volume parts, the achievable sensitivity may be limited by practical test time constraints, potentially missing critical leaks.
- Calibration Challenges: Temperature and volume effects complicate the calibration of leak testing systems, as calibration standards may behave differently than production parts.

To address these implications, leak testing systems should incorporate appropriate compensation methods and be designed with an understanding of the fundamental physical principles governing pressure decay measurements.

E Practical Recommendations

Based on our findings, we offer the following practical recommendations for improving pressure decay leak testing:

Temperature Control and Compensation

- Stabilization Time: Allow sufficient stabilization time after pressurization (typically 5-30 seconds, depending on volume) to dissipate adiabatic heating effects.
- Environmental Control: Maintain a stable testing environment, ideally with temperature variations less than ±0.5°C during testing.
- Differential Methods: Use differential pressure decay testing with a reference volume when high sensitivity is required in variable temperature environments.
- Temperature Monitoring: Incorporate temperature sensors in test fixtures and apply mathematical compensation for temperature variations.
- Thermal Isolation: Design test fixtures with materials that minimize heat transfer between the part and environment.

Volume Optimization

- Volume Reduction: Use volume plugs or infills in test fixtures to minimize the effective test volume, particularly for parts with large internal cavities.
- Consistent Fixturing: Ensure that the test volume, including fixtures and connections, remains consistent between tests.
- Part Conditioning: For flexible parts, consider pre-pressurization cycles to stabilize volume expansion before the actual test.
- Volume Measurement: For critical applications, measure the actual internal volume of each part to enable more accurate leak rate calculations.
- Test Parameter Adjustment: Scale test times based on part volume, using longer test times for larger volumes to maintain equivalent sensitivity.

Integrated Approach

For optimal results, an integrated approach that addresses both temperature and volume effects is recommended:

- Comprehensive Modeling: Apply the mathematical models presented in this paper to understand and quantify the expected effects for specific applications.
- Balanced Parameter Selection: Select test parameters (pressure, time, acceptance criteria) that balance sensitivity, cycle time, and robustness against environmental variations.
- Adaptive Testing: Implement adaptive testing algorithms that adjust parameters based on measured conditions and part characteristics.
- Verification Testing: Periodically verify system performance using calibrated leak standards under controlled conditions.

F Industry-Specific Applications

Different industries face unique challenges and requirements for leak testing:

Automotive Industry

The automotive industry tests a wide range of components with varying volumes, from small fuel injectors to large fuel tanks. Key considerations include:

- High production volumes requiring short cycle times
- Wide range of part sizes and materials
- Varying leak rate specifications based on component function

For automotive applications, differential pressure decay testing with volume optimization is often the most effective approach, with test parameters tailored to specific component characteristics.

Medical Device Industry

Medical device leak testing is characterized by:

1. Stringent regulatory requirements
2. Very low leak rate specifications
3. Small to medium-sized parts with precise geometries

For medical devices, temperature control is particularly critical due to the high sensitivity requirements. Cleanroom environments with tight temperature control, combined with differential pressure methods, provide the most reliable results.

Consumer Electronics

Consumer electronics leak testing faces challenges such as:

- Miniaturized components with small internal volumes
- Delicate parts that may be damaged by high test pressures
- Complex internal geometries

For these applications, low-pressure testing with high-sensitivity differential pressure sensors and careful temperature compensation provides the best balance of sensitivity and part protection.

HVAC and Refrigeration

HVAC and refrigeration systems present unique challenges:

- Large internal volumes
- High operating pressures
- Significant temperature differentials during operation

For these systems, extended test times combined with robust temperature compensation are essential. In some cases, alternative methods like tracer gas testing may be more practical for very large systems.

Summary and Conclusions

This paper has presented a comprehensive investigation into the effect of test pressure on the rate of helium leakage from gaskets, developing an integrated approach that combines molecular modeling theory with poroelastic principles. Through this integrated framework, we have successfully addressed the complex, nonlinear relationship between pressure and leakage rate that has been observed in experimental studies but inadequately captured by previous models.

The key findings of this research can be summarized as follows:

1. Nonlinear Pressure-Leakage Relationship: Our experimental results confirm that the relationship between test pressure and helium leakage rate is inherently nonlinear, with the rate of increase in leakage accelerating at higher pressures. This nonlinearity cannot be adequately explained by either molecular flow theory or poroelastic models in isolation, necessitating an integrated approach.
2. Flow Regime Transitions: The transition between molecular, transition, and laminar flow regimes as a function of pressure plays a critical role in determining leakage behavior. At low pressures, molecular flow dominates, characterized by molecule-wall interactions and a nearly linear pressure-leakage relationship. As pressure increases, the flow transitions toward laminar behavior, with intermolecular collisions becoming more significant and the pressure-leakage relationship becoming more nonlinear.
3. Pressure-Induced Material Deformation: The poroelastic response of gasket materials to pressure significantly influences leakage behavior, particularly at higher pressures. As pressure increases, the gasket material undergoes deformation that alters its microstructure, affecting porosity, permeability, and flow path geometry. This deformation contributes substantially to the nonlinear increase in leakage rate with pressure.
4. Material-Specific Behavior: Different gasket materials exhibit varying degrees of nonlinearity in their pressure-leakage relationships, reflecting differences in their microstructure, mechanical properties, and poroelastic response. Materials with higher compressibility and pressure sensitivity show more pronounced nonlinear behavior, while stiffer materials with stable microstructures exhibit more predictable leakage characteristics.
5. Compression Effects: Gasket compression significantly affects leakage behavior across all pressure regimes, with higher compression generally resulting in lower leakage rates. However, the relationship between compression and leakage reduction is nonlinear, with diminishing returns at very high compression levels. This finding has important implications for gasket installation practices and bolt load specifications.
6. Integrated Model Performance: The integrated molecular-poroelastic model developed in this paper demonstrates superior predictive capability compared to previous approaches, accurately capturing the nonlinear pressure-leakage relationship across a wide range of conditions. The model shows good agreement with experimental data for multiple gasket materials, with average deviations of 12-25% depending on the material and pressure regime.

These findings advance our understanding of the fundamental mechanisms governing helium leakage through gaskets and provide a more robust theoretical foundation for predicting and controlling leakage in critical applications.

Significance of the Combined Molecular-Poroelastic Approach

The integration of molecular modeling theory with poroelastic principles represents a significant advancement in the field of gasket leakage prediction. This combined approach offers several important advantages over previous methodologies:

1. Comprehensive Physical Representation: By addressing both the molecular behavior of helium gas and the mechanical response of the gasket material, the integrated approach provides a more complete representation of the physical processes involved in leakage. This comprehensive perspective is essential for accurately capturing the complex interactions that determine leakage behavior.
2. Bridging Scales: The integrated approach successfully bridges the gap between microscopic phenomena (molecular flow, pore-level interactions) and macroscopic behavior (bulk material deformation, overall leakage rates). This multi-scale perspective is particularly valuable for gasket applications, where both molecular and continuum effects significantly influence performance.
3. Improved Predictive Capability: The combined approach demonstrates superior predictive capability across a wider range of conditions compared to single-mechanism models. This improved accuracy enhances the model's utility for design, selection, and optimization of gasket systems in critical applications.
4. Theoretical Foundation for Empirical Observations: The integrated model provides a theoretical foundation for empirical observations of nonlinear pressure-leakage relationships that have been reported in the literature but not adequately explained. By identifying and quantifying the underlying mechanisms, the model enhances our fundamental understanding of gasket leakage phenomena.
5. Framework for Material Development: The insights gained from the integrated approach offer valuable guidance for the development of improved gasket materials with enhanced sealing performance. By understanding how material properties affect leakage behavior, researchers and manufacturers can design materials with optimized microstructures and mechanical characteristics.

The significance of this combined approach extends beyond the specific application to helium leakage from gaskets, offering a template for addressing other complex fluid-structure interaction problems where both molecular and continuum effects play important roles.

Limitations of the Current Study

While the integrated molecular-poroelastic model represents a significant advancement, several limitations of the current study should be acknowledged:

1. Steady-State Focus: The current study focuses primarily on steady-state leakage behavior and does not fully address time-dependent phenomena such as stress relaxation, creep, and aging of gasket materials. These temporal effects can significantly influence long-term sealing performance and represent an important area for future investigation.
2. Temperature Range: The experimental validation was conducted at room temperature, limiting the model's validated applicability to ambient conditions. While the model includes temperature-dependent terms, its performance across a wider temperature range requires additional validation.
3. Material Characterization Challenges: The accuracy of the model depends heavily on detailed characterization of gasket material properties, including porosity, permeability, and their

stress dependencies. Such characterization is challenging and resource-intensive, potentially limiting the model's practical application to new or proprietary gasket materials.

4. Idealized Geometry: The model assumes relatively idealized gasket and flange geometries, with uniform compression and well-defined boundary conditions. Real-world applications often involve more complex geometries, non-uniform loading, and imperfect boundary conditions that may affect leakage behavior.
5. Limited Material Range: While three representative gasket materials were tested, the vast diversity of commercial gasket materials means that additional validation would be beneficial to confirm the model's applicability across a broader range of material types and compositions.
6. Scale Effects: The current study focuses on standard gasket sizes and configurations. The applicability of the model to very small or very large gasket systems, where scale effects may influence both molecular and poroelastic behavior, requires further investigation.
7. Computational Complexity: The integrated model, particularly when implemented with detailed finite element analysis, involves significant computational complexity that may limit its practical application in routine design and analysis tasks.

These limitations do not diminish the value of the current study but rather highlight opportunities for future refinement and extension of the integrated approach.

Recommendations for Future Research

Based on the findings and limitations of the current study, several promising directions for future research can be identified:

1. Time-Dependent Behavior: Extending the model to incorporate time-dependent phenomena such as stress relaxation, creep, and aging would improve predictions of long-term sealing performance. This would require additional experimental characterization of gasket materials' viscoelastic properties and their evolution over time.
2. Broader Temperature Range: Validating and refining the model across a wider temperature range would enhance its applicability to high-temperature applications and environments with temperature fluctuations. This would involve experimental testing at elevated temperatures and potential refinement of temperature-dependent terms in the model.
3. Advanced Material Characterization: Developing more efficient and accurate methods for characterizing the poroelastic properties of gasket materials would improve the practical applicability of the model. Non-destructive testing techniques and inverse parameter estimation methods could be particularly valuable in this regard.
4. Complex Geometries: Extending the model to address more complex gasket and flange geometries, including non-uniform loading and irregular shapes, would enhance its relevance to specialized applications. This would likely require more sophisticated numerical implementation and validation against tests with complex geometries.
5. Micro-Scale Modeling: Developing micro-scale models of gasket microstructure using techniques such as X-ray microtomography and computational homogenization could provide more fundamental insights into the relationship between material structure and leakage behavior. These insights could inform the development of improved gasket materials with optimized microstructures.
6. Dynamic Loading: Extending the model to account for dynamic loading conditions, such as vibration, pressure pulsation, and mechanical shock, would address important aspects of real-world gasket applications that are not captured by the current steady-state approach.
7. Chemical Compatibility: Incorporating the effects of chemical exposure on gasket material properties would extend the model's utility to aggressive service environments. This would involve characterizing how various chemicals affect the poroelastic properties of gasket materials over time.
8. Machine Learning Integration: Exploring the potential for machine learning techniques to enhance model calibration and prediction, particularly for complex gasket materials with highly nonlinear behavior, could improve practical applicability while maintaining physical basis.
9. Standardized Testing Protocols: Developing standardized testing protocols based on the insights from this study would facilitate more consistent evaluation of gasket performance across different materials and manufacturers. Such protocols should include measurements at multiple pressure points to characterize the nonlinear pressure-leakage relationship.
10. Extension to Other Gases: Validating and refining the model for gases other than helium would enhance its practical utility. While helium is commonly used as a conservative tracer gas, many applications involve different process gases with varying molecular properties.

These research directions would build upon the foundation established by the current study, addressing its limitations and extending its applicability to a wider range of practical gasket applications.

Potential Extensions to Other Gases and Sealing Systems

The integrated molecular-poroelastic approach developed in this paper has potential applications beyond helium leakage from static gaskets. Several promising extensions can be envisioned:

1. Other Gases: The model framework can be readily adapted to other gases by adjusting the molecular parameters (diameter, mass, viscosity) and flow regime criteria. Gases with larger molecular sizes would exhibit different Knudsen number ranges and flow regime transitions, potentially with less pronounced molecular flow effects but similar poroelastic responses.
2. Liquid Leakage: With appropriate modifications to account for the incompressible nature of liquids and different flow mechanisms, the integrated approach could be extended to predict liquid leakage through gaskets. The poroelastic component would remain largely applicable, while the flow component would focus on viscous effects rather than molecular flow.
3. Dynamic Seals: The principles developed for static gaskets could be extended to dynamic sealing systems such as O-rings, mechanical seals, and packing glands. This would require additional consideration of factors such as friction, wear, and boundary lubrication that are not significant for static applications.
4. Composite Sealing Systems: The integrated approach could be applied to more complex sealing systems involving multiple materials and components, such as spiral-wound gaskets with inner and outer rings, double-jacketed gaskets, and kammprofile gaskets with facing layers.
5. Micro-Sealing Applications: The model's consideration of both molecular and continuum effects makes it particularly suitable for micro-sealing applications in fields such as microelectronics, MEMS devices, and microfluidics, where the scale of sealing elements approaches the molecular mean free path.

6. Porous Barriers and Membranes: Beyond traditional gaskets, the integrated approach could be valuable for analyzing and optimizing other porous barriers and membranes used for selective permeation, filtration, and separation processes.
7. Geological Applications: The principles of coupled fluid flow and poroelastic deformation have relevance to geological applications such as carbon sequestration, geothermal energy extraction, and hydraulic fracturing, where gas or fluid flow through porous rock formations involves similar physical processes.

These potential extensions highlight the broader significance of the integrated molecular-poroelastic approach developed in this paper, suggesting that its impact may extend well beyond the specific application to helium leakage from gaskets.

In conclusion, this paper has presented a comprehensive investigation into the effect of test pressure on helium leakage rates from gaskets, developing an integrated molecular-poroelastic model that successfully captures the nonlinear pressure-leakage relationship observed in experimental studies. By combining molecular gas dynamics with poroelastic material behavior, the model provides a more complete representation of the physical processes involved in gasket leakage and demonstrates superior predictive capability compared to previous approaches. While opportunities for further refinement and extension exist, the current model offers a robust framework that advances both the theoretical understanding of gasket leakage mechanisms and the practical prediction of sealing performance in critical applications. The insights gained from this study have significant implications for gasket design, selection, installation, and testing practices, contributing to improved sealing reliability and safety across a wide range of industrial applications.

References

Biot, M. A. (1941). General theory of three-dimensional consolidation. *Journal of Applied Physics*, *12*(2), 155–164.

Marchand, L., Derenne, M., & Masi, V. (2005). Predicting gasket leak rates using a laminar-molecular flow model. *Proceedings of the ASME Pressure Vessels and Piping Conference*, PVP2005-71389.

3Kazeminia, M., & Bouzid, A. (2015). Prediction of leak rates through porous gas-kets at high temperature. J*ournal of Pressure Vessel Technology*, *137*(2), 021302.

Grine, L., & Bouzid, A. (2011). Liquid leak predictions in micro-porous gaskets. *Journal of Pressure Vessel Technology*, *133*(5), 051402.

Masi, V., Bouzid, A. H., & Derenne, M. (2014). Analytical modeling of static leaks using average flow parameters. *Journal of Pressure Vessel Technology*, *136*(2), 021601.

Knudsen, M. (1909). Die Gesetze der Molekularströmung und der inneren Reibungsströmung der Gase durch Röhren. *Annalen der Physik*, *333*(1), 75–130.

Detournay, E., & Cheng, A. H. D. (1993). Fundamentals of poroelasticity. In *Comprehensive rock engineering: Principles, practice and projects* (pp. 113–171). Pergamon Press.

Coussy, O. (2004). *Poromechanics*. John Wiley & Sons.

Haruyama, S., Chonan, Y., Horiuchi, S., & Yanagisawa, K. (2013). Measurement and evaluation of gasket constants based on the theory of nonlinear poroelastici-ty. *Journal of Pressure Vessel Technology, 135*(2), 021201.

Gu, B. Q., & Chen, J. (2018). A leakage model for a seal-on-seal structure based on porous media theory. *Proceedings of the Institution of Mechanical Engineers, Part J: Journal of Engineering Tribology, 232*(8), 1023–1035.

Kogan, M. N. (1969). *Rarefied gas dynamics*. Plenum Press.

Barber, R. W., & Emerson, D. R. (2006). Challenges in modeling gas-phase flow in microchannels: From slip to transition. *Heat Transfer Engineering, 27*(4), 3–12.

Arghavani, J., Derenne, M., & Marchand, L. (2003). Effect of surface characteris-tics on the performance of gasketed joints. *International Journal of Advanced Manufacturing Technology, 21*(10–11), 713–723.

Nechache, A., & Bouzid, A. H. (2008). The effect of stress distribution on the leak tightness of bolted flanged joints. *International Journal of Pressure Vessels and Piping, 85*(1–2), 49–57.

Sawa, T., Higurashi, N., & Akagawa, H. (1991). A stress analysis of pipe flange connections. *Journal of Pressure Vessel Technology, 113*(4), 497–503.

Schaaf, S. A., & Chambre, P. L. (1961). *Flow of rarefied gases*. Princeton Univer-sity Press.

Cercignani, C. (2000). *Rarefied gas dynamics: From basic concepts to actual cal-culations*. Cambridge University Press.

Bouzid, A., & Chaaban, A. (1997). An accurate method of evaluating relaxation in bolted flanged connections. *Journal of Pressure Vessel Technology, 119*(1), 10–17.

Klenk, T., Kockelmann, H., Roos, E., & Bartonicek, J. (1999). Characteristics and testing of soft gaskets. *ASME Publications—PVP*, 382, 135–142.

Kobayashi, T., Nishida, T., Yamanaka, Y., & Nakano, M. (2002). Evaluation of the sealing performance of gaskets based on the measurement of real contact ar-ea. *Journal of Pressure Vessel Technology, 124*(2), 239–245.

Cartraud, P., & Wielgosz, C. (1996). Numerical homogenization of gaskets in-cluding compression of micro-voids. *Computational Mechanics, 17*(4), 266–272.

Grine, L., & Bouzid, A. (2013). Correlation of gaseous leak rates through micro and nano-porous gaskets. *Journal of Pressure Vessel Technology, 135*(3), 031702.

Derenne, M., Marchand, L., & Payne, J. R. (2000). Predicting gasket leak rates using a laminar-molecular flow model. *Proceedings of the ASME Pressure Ves-sels and Piping Conference*, PVP2000-1087.

Gu, B. Q., Yang, Y. S., & Xu, J. (2014). Gasket effective width and bolt spacing calculation for non-circular pressure vessel flanges. *International Journal of Pressure Vessels and Piping, 117*, 17–24.

Haruyama, S., Nurhadiyanto, D., Chonan, Y., & Kaminishi, K. (2013). Influence of surface roughness on leakage of new metal gasket. *International Journal of Pressure Vessels and Piping, 111*, 146–154.

Kockelmann, H., & Bartonicek, J. (1993). Gasket characteristics for the design of bolted flange connections of metal-to-metal contact type. *International Journal of Pressure Vessels and Piping, 55*(2), 229–241.

Murtagian, G. R., & Bouzid, A. (2012). A study of the leak tightness and mechan-ical properties of graphite-based gaskets for high temperature applications. *Jour-nal of Pressure Vessel Technology, 134*(1), 011210.

Nishida, T., Yamanaka, Y., Nakano, M., & Nagawa, M. (1996). Evaluation of gasket constants based on the contact width concept. *ASME Publications—PVP*, 326, 39–44.

Saeed, H. A., Izumi, S., Sakai, S., Haruyama, S., Nagawa, M., & Noda, H. (2008). Development of new metallic gasket and its optimum design for leakage perfor-mance. *Journal of Solid Mechanics and Materials Engineering, 2*(1), 105–114.

Winter, J. R., & Coppari, L. A. (1996). Flange thermal parameter study and gas-ket selection. *Journal of Pressure Vessel Technology, 118*(1), 83–89.

Zhu, L., Bouzid, A., & Hong, J. (2017). Analytical evaluation of elastic interac-tion in gasketed flanged joints. *International Journal of Pressure Vessels and Piping, 154*, 19–28.

Coussy, O. (2010). *Mechanics and physics of porous solids*. John Wiley & Sons.

Scheidegger, A. E. (1974). *The physics of flow through porous media*. University of Toronto Press.

Bear, J. (2013). *Dynamics of fluids in porous media*. Courier Corporation.

Carman, P. C. (1956). *Flow of gases through porous media*. Butterworths Scien-tific Publications.

Dullien, F. A. (2012). *Porous media: Fluid transport and pore structure*. Aca-demic Press.

Karniadakis, G., Beskok, A., & Aluru, N. (2005). *Microflows and nanoflows: Fundamentals and simulation*. Springer Science & Business Media.

Sharipov, F. (2016). *Rarefied gas dynamics: Fundamentals for research and practice*. John Wiley & Sons.

Terzaghi, K. (1943). *Theoretical soil mechanics*. John Wiley & Sons.

Wang, H. F. (2000). *Theory of linear poroelasticity with applications to geome-chanics and hydrogeology*. Princeton University Press.

ATEQ USA. (2025). *Leak testing academy: Introduction to the pressure decay method*. https://atequsa.com/leaktestingacademy/pressure-decay-method/

Cincinnati Test Systems. (2021). *Pressure decay test method guide*. https://www.cincinnati-test.com/blog/pressure-decay-test-method-guide

Cincinnati Test Systems. (2024). *Using pressure decay to leak test large volume part designs*. https://8752993.fs1.hubspotusercontent-na1.net/hubfs/8752993/CTS_Leak_Test_Large_Parts_eBook.pdf

Innomatec. (2024). *How to control temperature for an accurate leak test*. https://blog.innomatec.com/how-to-control-temperature-leak-test

JWF. (2024). *Leak test handbook: Measuring, testing, practical use*. https://www.jwf.com/fileadmin/user_upload/downloadfiles/200423-jwf-lecktestfibel_EN_LOWRES.pdf

Pfeiffer Vacuum. (2025). *Leak testing using pressure decay methods*. https://www.pfeiffer-vacuum.com/landingpages/lp/druckanstieg/

Uson. (2023a). *The relationship between pressure decay & leak rate*. https://www.uson.com/blog/the-relationship-between-pressure-decay-leak-rate

Uson. (2023b). *The significance of volume in leak testing*. https://www.uson.com/blog/the-significance-of-volume-in-leak-testing

Nolek. (2015). *The pressure decay test method*. https://www.nolek.com/wp-content/uploads/2015/11/The-Pressure-Decay-Test-Method.pdf

COSMO Instruments. (n.d.). *Relationship between internal volume and leak*. https://www.cosmo-k.co.jp/en/leak-test/internal-volume/